MATERIALS CHEMISTRY FRONTIERS

REVIEW

View Article Online
View Journal | View Issue

Cite this: *Mater. Chem. Front.*, 2026, **10**, 1536

Hydrogel ionic sensory systems

Rui Chen,[ac] Rongxi Guo,[c] Ying Li,[c] Hao Yan,[c] Jin Huang,[c] Hexiang Xu,[c] Wei Shi,[ac] Zongzheng Zhang,[a] Shuyun Zhuo*[b] and Mingjie Liu *[abc]

Received 26th January 2026,
Accepted 12th April 2026

DOI: 10.1039/d6qm00061d

rsc.li/frontiers-materials

When interacting with the dynamic world, creatures always outdo their electronic counterparts because of their sophisticated sensory systems. From direct perception of the world *via* soft tissue to intelligent information processing, immensely varied biological movements of organisms mostly rely on accurate ion transport. Imitating the flexible structure of biological systems and the functional mechanism based on ion transport would essentially solve the unmet needs of modern sensing technology. Simultaneously, the establishment of ionic sensor systems would effectively narrow the gap between the biological systems and the artificial equipment to promote seamless interaction of both sides, which could bring a revolution in advanced operations and medical rehabilitation. The outstanding properties of hydrogels enable them to be used as ion conductors like biological tissues for the development of ionic sensory systems. In this review, we introduce the basic principles of ion transport in hydrogels, and discuss the five key elements of hydrogel ionic sensory systems: ionic sensors, ionic transporters, ionic processors, ionic effectors, and ionic power sources, in terms of their structures, working mechanisms and applications. Finally, we suggest future directions and potential challenges of hydrogel-based ionic sensory systems.

1. Introduction

Perception connects creatures with the real world. In the process of continuous evolution, organisms have gradually mastered more efficient ways to sense and modulate signals. By using multiple sensors, humans receive external stimuli and convert them into ionic electrical signals. The ionic signals propagate along afferent neurons to central nerves for information processing and interpretation, and then output nerves feedback the signals to effectors to complete a perception–response loop to the external stimulus. The coordinated and sophisticated sensor systems help humans interact harmoniously with the colorful world. The precise migration of ions is the basis for most biological processes including the complete sensing process. In contrast, the sensory systems in modern equipment are mainly based on electronic transport.[1–3]

[a] *State Key Laboratory of Bioinspired Interfacial Materials Science, Bioinspired Science Innovation Center, Hangzhou International Innovation Institute, Beihang University, Hangzhou 311115, China. E-mail: liumj@buaa.edu.cn*
[b] *International Institute for Interdisciplinary and Frontiers, Beihang University, Beijing 100191, China. E-mail: zhuosy@buaa.edu.cn*
[c] *State Key Laboratory of Bioinspired Interfacial Materials Science, School of Chemistry, Beihang University, Beijing, China*

Rui Chen

Dr Chen is currently a postdoctoral researcher at Beihang University. His research is focused on the precise design and structure–property relationships of heterogeneous hydrogels.

Rongxi Guo

Rongxi Guo received his BS degree in chemistry from the School of Chemistry and Chemical Engineering, Shandong University in 2025. He is currently pursuing his MS degree at the School of Chemistry, Beihang University, under the supervision of Prof. Mingjie Liu. His current research is focused on multi-network hydrogels and hydrogel lubricating coatings.

At present, machine sensory systems rely on rigid and bulky electronic sensing devices to obtain information from the outside world, which cannot collect high-quality data on irregularly curved and dynamic surfaces while providing timely motion feedback.[4,5] Simultaneously, electronic based information processing technology is subject to the physical limitations predicted by Moore's Law, and it is difficult to further reduce the size on the basis of nanoscale devices to improve performance.[6,7] Therefore, machines that rely on electronic microprocessors for signal processing face the problems of high power consumption and insufficient processing capabilities with the explosive growth of data. This is a far cry from the performance of an accurate, efficient, and low-energy (a power consumption on the order of several fJ per spike) biosensing system.[8–12]

Inspired by the powerful information acquisition and processing capabilities of organisms, researchers have invested enormous effort in the development of bionic electronic devices to break the barriers to the development of electronic equipment.[13–30] However, according to the current general consensus, the development of technology to help electronic products achieve advanced information transmission is difficult,[6] because there are fundamental differences in both working principles and composition between traditional electronic devices and biological systems.[31–34] Electronics has a constant architecture in terms of information acquisition and processing. In contrast, creatures use abundant sensors and soft physiological structures to sensitively feel environmental stimuli and provide timely action feedback. The transmission of the signals is completed by stimulus-induced ion transport across cell membranes. The transport of ions across membranes involves passive transport by ion channels or active transport by ion pumps, ion pumps and ion channels with the ability to selectively transport ions, which make ion migration more controllable in terms of ion species, direction, and speed.[35,36] Simultaneously, through bidirectional communication between pre-synaptic and post-synaptic neurons, synapses dynamically modulate weight to realize the adaptive decision-making of organisms to the environment.[8] Its superior perception and information processing ability are the inherent benefits of the adaptive, plastic network of sensory neurons. Hence, simulating biological processes from the level of sensing structure and mechanism would fundamentally realize biological-like perception.

A hydrogel is a water-rich polymer, and its high similarity with biological tissue makes it an ideal material for preparing ionic sensory systems.[37,38] Hydrogel ionic sensory systems realize their functions through ionic motion and arrangement.[39,40] The high water content of a hydrogel enables it to carry mobile ions for signal transmission. Moreover, contained ions can significantly increase the conductivity of a hydrogel to $\sim$10 S m^{-1} for sensing and signal transmission.[41,42] Since there are two types of ions with opposite charges in nature, the selective migration of ions and the local accumulation of anions and cations can be achieved by adjusting the electrostatic groups carried by the hydrogels. This means that the computing power of ion hydrogel-based information processors may be unparalleled.

An elastic polymer network offers the possibility of making flexible, stretchable ionic conductor equipment. The elastic modulus of hydrogels is in the range of 1–100 kPa, which is close to the softness of human tissue.[43,44] At the same time, it can withstand large deformations.[45] However, changes in the configuration of a polymer network and water molecules rarely affect ionic conductivity.[46] Hence, hydrogel-based sensing elements can tightly combine with the target and work normally in a stretched state, for example, a hydrogel sensor can compliantly attach to dynamic and irregular objects to obtain high-fidelity data acquisition. On the other hand, the transmission and distribution of ions sensitively respond to changes in

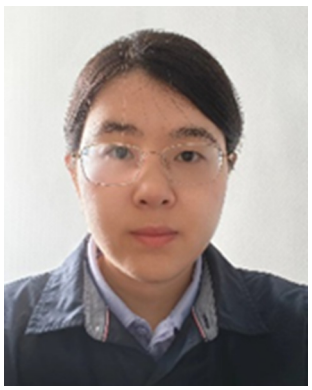

Shuyun Zhuo

Dr Zhuo is primarily engaged in the research of bioinspired multifunctional hydrogels and their applications in flexible electronics and soft robotics. By designing orthogonal supramolecular heterogeneous networks, she has developed mechanically programmable hydrogel materials featuring multiple mechanically tunable properties, dual shape/stiffness memory, biocompatibility, self-healing capability, and adhesion. She has published 18 papers in international academic journals including Nature Communications, Science Advances, and Advanced Materials, with a total citation count exceeding 900.

Mingjie Liu

Prof. Mingjie Liu is a professor at Beihang University, with postdoctoral experience at RIKEN, Japan (2010–2015). His research is focused on bio-inspired functional polymer composites, designing high-performance elastomers through multiphase synergy and ordered structures for soft robotics, wearable devices, and antifouling drag reduction. He has authored papers in prestigious journals including Nature, Nature Reviews Materials, Nature Communications, Science Advances, Angewandte Chemie, Advanced Materials, and JACS.

the geometry of a polymer network and the environment, thus giving the ionic hydrogel a powerful sensing function.[47,48] At the same time, the configuration of the polymer would also be affected by the transmission and distribution of ions under the action of an electric field, which endows the hydrogel with electrical actuation functions.

The polymer network does not scatter light, as a hydrogel with high water content (60–90 wt%) usually shows a refractive index (1.333) and transmittance as high as ~99% similar to water.[49,50] More importantly, because devices of hydrogel ionic sensory systems normally consist of non-toxic hydrogels, those applications are much less restricted in terms of biocompatibility, biodegradability, and ecological requirements. These fascinating properties make the development of hydrogel ionic sensory systems highly anticipated.

Herein, we discuss five essential components of hydrogel ionic sensory systems: ionic sensors for signal reception, ionic transporters for signal transmission, ionic processors for signal interpretation and processing, ionic effectors for signal feedback, and ionic power sources for energy supply (Fig. 1). We focus on device structures, working mechanisms, functions, and potential applications. Prior to this, the transport mode, modulation mode, the mechanism of transport of ions in hydrogels, and the method to improve the charge transport in the hydrogel were elaborated to better understand the working principle of hydrogel-based sensory system components. In addition, future directions and key challenges related to hydrogel-based devices are proposed.

2. Transport of ions in hydrogels

In biological systems, transmission of information is closely linked to accurate ion migration. Based on the understanding of the physicochemical properties of both ions and hydrogels, and the mechanisms of ion transport in hydrogels to carefully design components, ion migration in the hydrogel ionic sensor systems would be more controllable in terms of direction, velocity, and type.

2.1. Mode of ion transport

According to the types of ions that can move freely in the electric field, ion transport is divided into two forms: the transport mode in which both anions and cations can migrate in the electric field is called non-selective ion transport. Under the action of an electric field, cations move to the negative electrode, and anions move to the positive electrode (Fig. 2a). But in selective ion transport, only one type of ions can pass through ion-selective materials. The selective transport of ions can be achieved by polyelectrolyte hydrogels, which are composed of fixed polymer chains with charges and counterions with opposite charges (Fig. 2b).[51] When the electric field is applied, counterions migrate directionally, and the polymer chains hinder the entry of ions with the same charges as them. More complex information processing and sensing functions can be achieved through accurate ion transportation.

2.2. Mode of ion modulation

There are two mechanisms involved in modulating ions in hydrogels: a capacitive process and a faradaic process. In the

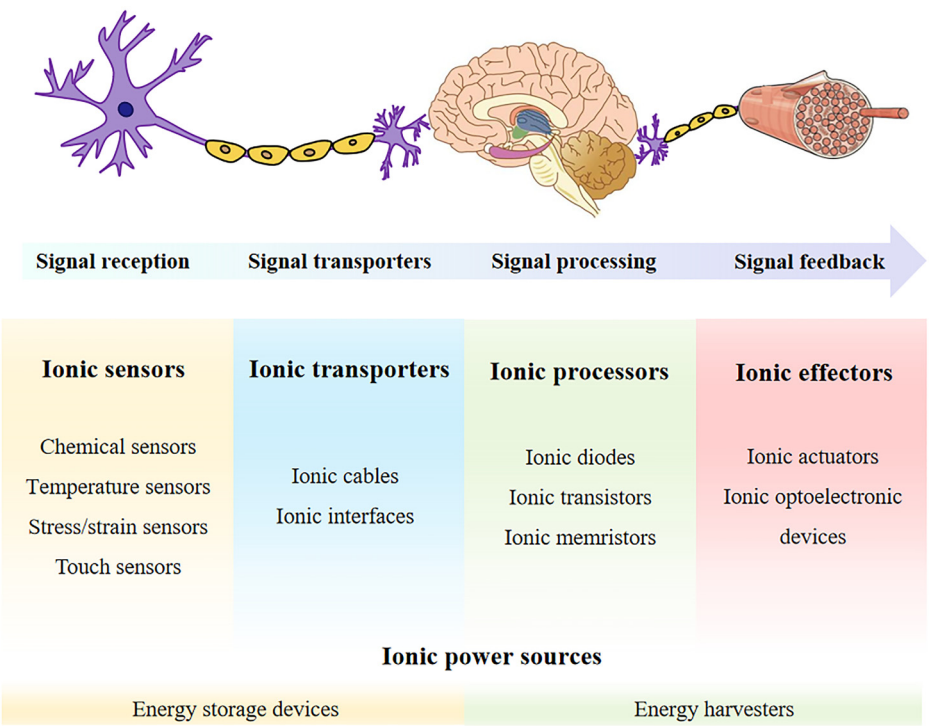

Fig. 1 Overview of perception–response loop of hydrogel ionic sensory systems.

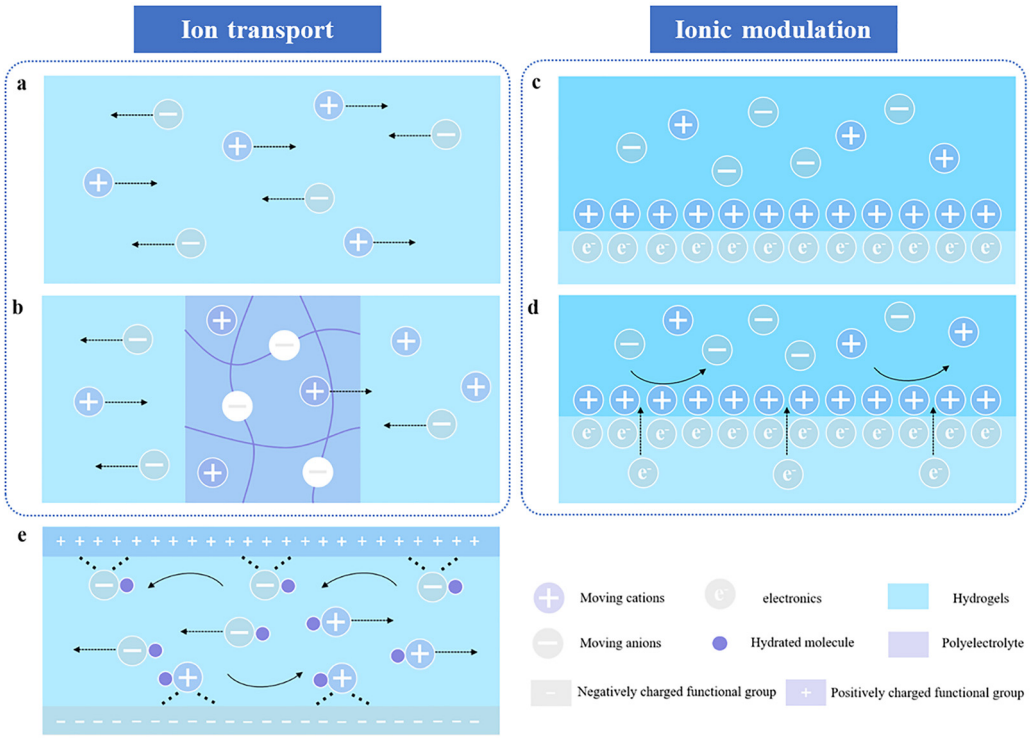

Fig. 2 Transport of ions in hydrogels. (a and b) Schematic illustration of two modes of ion transport: (a) in non-selective ion transport, both anions and cations can move directionally through an electric field; (b) schematic diagram of selective ion transport, such as a cation selective system, in which only cations can be transported through a selective membrane. (c and d) Two types of ionic modulation: (c) schematic illustration of the electrical double layer (EDL) formation. Cations and electrons accumulate on both sides of the interface between the hydrogel and the electrode, respectively. (d) Schematic illustration of the Faradaic process. Electrons participate in redox reactions through charge transfer at the electrode/hydrogel interface. (e) Schematic illustration of the transport process of ions in the hydrogel. The transport process involves solvation of ions and polymer–ion interactions.

capacitance model, ions and electrons accumulate at the interface between hydrogels and metal electrodes to form an electric double layer (EDL) for signal transmission and detection (Fig. 2c). The faradaic process involves redox reactions in which electrons are transferred between different substances (Fig. 2d).[52]

2.3. Ion conductivity

The ion transport capacity of hydrogels is quantified by ion conductivity, which is the core performance of a hydrogel as an ion conductor. Ion conductivity σ reflects the solvation/dissociation and migration of ions, in terms of the free ion number n_i and the ionic mobility μ_i:[53]

$$\sigma = \sum n_i \mu_i Z_i e$$

where Z_i is the valence order of the ion, and e is the unit charge of electrons. The concentration and mobility of carriers are related to the concentration of salts, type of salts, and the properties of the polymer. We will discuss methods to improve the ion conductivity of hydrogels in terms of the following aspects:

Salt concentration. A reasonable increase in the concentration of electrolyte salts would bring more charge carriers to increase the conductivity. However, after a certain salt concentration, the system exhibits a high viscosity that is harmful to ion migration, resulting in a decrease in ion conductivity.[54,55] Further increasing the salts content would cause the ions to be unable to dissolve completely and even show the nature of the solid.

Ionic types. An ion exists in the form of a hydrate ion in aqueous electrolyte, not in the form of a single ion.[56,57] Reducing the hydrated water molecules around ions to increase the concentration and migration speed of carriers is an effective strategy to improve ion conductivity. Metal cations with higher charge density tend to attract more water molecules, thereby reducing ion mobility.[58,59] For example, the charge density of a monovalent cation decreases with increasing ionic radii and its ionic conductivity is directly proportional to the charge density.[60] The same pattern is also exhibited in anions. Another example, bulky-anions can effectively reduce the number of water molecules around the cations, thereby promoting the generation and transportation of cations.[61] For example, compared with $ZnSO_4$, $Zn(CF_3SO_3)_2$ is more beneficial to Zn^{2+} conduction.

Medium of ion transport. Ions are transported through the polymer network and water in a hydrogel (Fig. 2e). The hydrophilic functional groups of the polymer can bond with water molecules through non-covalent interactions (such as hydrogen bonds and electrostatic interactions). According to the strength

of the interaction with the polymer chains, water can be divided into three types, namely bound water, intermediate water and free water.[62,63] The interaction with polymer chains of free water is negligible. The mesh of the polymer network is much larger than that of water molecules, so the water can maintain similar properties to bulk water. The high dielectric constant ($\varepsilon = 80$) and the low viscosity of water (1 cP at 20 °C) facilitate the solvation of ions and increase ionic mobility.

The polymer network provides an elastic backbone for a hydrogel, but it is an insulator. Compared with liquid electrolytes, the ionic conductivity of a hydrogel containing electrolytes would decrease significantly. Therefore, the hindrance of the polymer to ion migration should be reduced. For instance, reducing the mass fraction of the polymer can effectively improve conductivities.[64–66] On the other hand, hydrogels have a porous structure. These pores of tens of nanometers allow water molecules to move freely and provide abundant channels for ion transport. So, enlarging the pore size of hydrogels is beneficial to ion transmission.[67,68] As an example, a nanofibrillated cellulose/polyacrylamide hydrogel with enlarged pore sizes *via* nanofibrillated cellulose as a synthesis template has significantly improved ionic conductivity. As pore sizes are enlarged from 20–40 μm to 60–80 μm, the ionic conductivity also increases from 16.9 to 22.8 mS cm^{-1}.[67] Another example, using hydroxypropyl cellulose to expand the pore size significantly increased the conductivity of the hydroxypropyl cellulose/polyvinyl alcohol hydrogel from 1.7 to 3.4 S m^{-1}.[68] It should be noted that although increasing the pore size can promote ion transport, this comes at the cost of sacrificing the mechanical integrity and structural stability of the hydrogel network.[69] Hydrogels with high porosity usually have poor mechanical durability and are prone to collapse due to dehydration, which limits their long-term applications.[70]

The functional groups carried by the polymer also can affect the migration behavior of the ions by interacting with the ions. As an important example, a zwitterionic electrolyte hydrogel composed of repeating units of anion and cation charged groups shows unique advantages in this regard. The rich charged groups can not only be very hydrated with water molecules to induce the hydrogel's strong water retention ability, but also provide hopping migration channels to greatly improve the ion conductivity.[71–73] In the meantime, the cation and anion charge on the same molecule can induce the dissociation of the introduced salt through electrostatic interaction, thereby increasing the number of free ions to improve conductivity.[74] The energy storage devices based on the outstanding advantages of the polyzwitterionic hydrogel electrolyte exhibit a remarkably impressive capacitance and rate capacity.[71,75,76]

Weakening the interaction between polymers and ions is also an effective way to improve ion conductivity.[77,78] For instance, decreasing the oxygen content in the polymer can reduce the coordination effect between Li^+ and the polymer, which leads to enhanced Li^+ conduction.[78] However, polymer–ion interactions present a delicate balance. Weakening coordination between polymer chains and ions improves ionic mobility, but excessively weak interactions may reduce ion selectivity and lead to poor signal fidelity.[79] In contrast, strong electrostatic interactions can enhance ion selectivity and dissociation, yet may introduce slower responses due to ion trapping.[80]

Besides, the Vogel–Tamman–Fulcher (VTF) relationship reveals the connection between T_g and ionic conductivity of a polymer: a polymer with a lower T_g has a higher ionic conductivity.[81–84] The amorphous feature of a hydrogel with lower crystallinity can effectively enhance the ionic conductivity due to the flexibility of chain segmental motion.[85] For example, introduced additives or polymer modifications have been used to reduce the crystallinity of hydrogels to increase ion conductivity.[65,86–89]

3. Hydrogel ionic sensors

Using sensors to receive external stimuli is the beginning of a sensing process. A sensor is a machine that converts detected signals into electric signals.[90,91] The human body harbors numerous sensors that enable us to perceive five delicate sensations, including hearing, sight, touch, taste, and smell.[49] Similarly, through careful design, hydrogel ionic sensors can be used to effectively monitor a wide range of signals and convert them into the desired signal output. Hydrogel ionic sensors rely on the high compliance of the hydrogels, changes in the spatial distribution and the movable speed of ions in order to work (Table 1).

Table 1 Comparison of the performance of different ionic sensors based on hydrogels, nanomaterials and liquid metals

Functional materials	Sensor types	Sensitivity	Sensing range	Stability (cycles)	Ref.
Hydrogels	Pressure sensors	3.06 kPa^{-1}	0–380 kPa	2000	Zhuo *et al.*[92]
	Strain Sensor	GF = 4.9	0–800%	3000	Cui *et al.*[93]
	Pressure sensors	0.013 kPa^{-1}	1.3 kPa–70 kPa	20 000	Pu *et al.*[94]
	Strain Sensor	GF = 2.26	1–300%	500	Wang *et al.*[95]
Nano materials	Gas sensor	0.24	1–40 ppm	>1000	Chen *et al.*[96]
	Strain sensor	GF ≥ 14 000	0–900%	2000	Yang *et al.*[97]
	Pressure sensor	2048 kPa^{-1}	100 kPa	1000	Tian *et al.*[98]
	Temperature sensor	0.142% $°C^{-1}$	25–50 °C	5000	Gandla *et al.*[99]
Liquid metals	Strain sensor	GF = 4.91	320%	500	Chen *et al.*[100]
	Tactile sensor	$(2–20) \times 10^{-3}$ kPa^{-1}	2–400 kPa	500	Yeo *et al.*[101]
	Pressure sensor	39% kPa^{-1}	25 kPa	6000	Zhang *et al.*[102]
	Strain sensor	GF = 8.35	0–120%	10 000	Yao *et al.*[103]

3.1. Chemical sensors

Hydrogel-based chemical sensors convert external chemical stimuli into visual electrical signals. Chemical sensors can be divided into two categories according to whether they react with the detected substances.

Chemical sensors that react with substances affect ion conductivity by changing the structure of the pores and the interaction with ions of the polymer. Inspired by the tongue, the astringency sensor was constructed by using polyacrylamide containing mucin and lithium chloride (LiCl).[77] When exposed to astringent compounds, the microporous hydrogel is converted into micro/nanoporous structures with hydrophobic aggregates due to the binding of the contained mucin to incoming molecules (Fig. 3a and b). This is conducive to shortening diffusion paths and frictionless sliding of ions, thus improving ion conductivity to detect astringent substances.

For chemical sensors that do not react with the detection substances, ionic hydrogels can respond to changes in humidity and gas composition, because these changes are closely related to the hindering effect of ion transport. This mechanism makes it possible to use ionic hydrogels as gas or humidity sensors. For example, NH_3 and NO_2 can form hydrogen bonds with the oxygenated functional groups of the polymer network and be effectively absorbed by the hydrogel. These

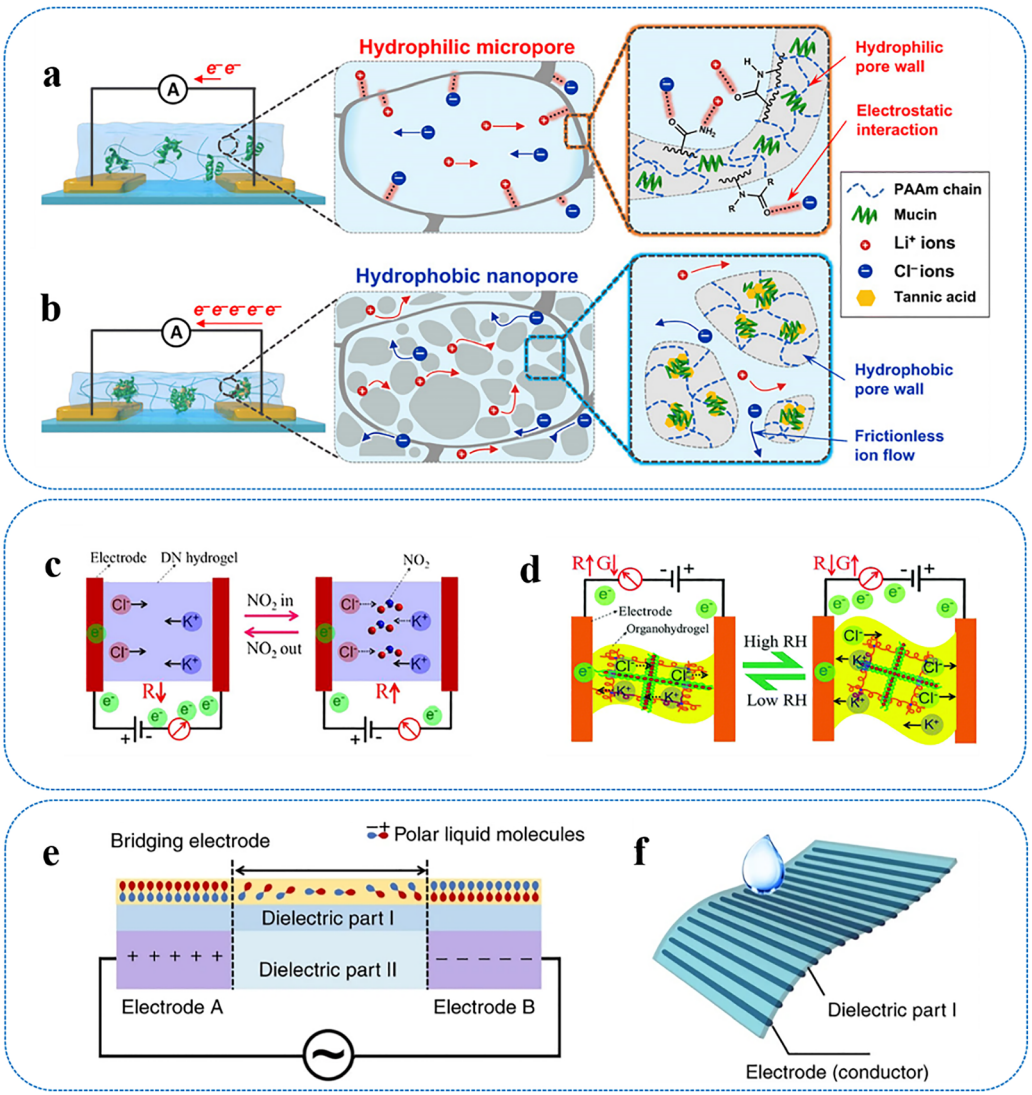

Fig. 3 Hydrogel ionic chemical sensors. (a and b) Schematic illustration of the working principle of an astringency sensor. (a) Before contacting astringent substances, the hydrogel has hydrophilic micropores and electrostatically charged pore walls that can limit ion transport.[77] (b) After making contact with astringent substances, the hydrogel exhibits hierarchical micro/nanopores that can shorten diffusion paths, and hydrophobic pore walls that can facilitate ion sliding.[77] (c) Schematic depicting the working mechanism of a NO_2 sensor. The NO_2 molecules absorbed by a hydrogel hinder the movement of ions and increase the resistance.[104] (d) Schematic illustrating of humidity sensing mechanism. The moisture in the air absorbed by a hydrogel reduces the density of the polymer network, thereby facilitating ion migration.[105] (e) Schematic illustration of a capacitive sensor for liquid recognition. Liquid acting as a bridging electrode would increase capacitance. The characteristics of the increased capacitance signals reflect the properties of the liquid.[106] (f) A 3D-pringting capacitive liquid recognition sensor.[106]

absorbed gases impede the movement of ions, resulting in an increase in resistance (Fig. 3c).[104] Hydrogels can also effectively absorb moisture in the air, and the increase in humidity can help hydrogels absorb more water and cause swelling. This reduces the density of the polymer network to alleviate the hindrance of ion migration, resulting in a decrease in the resistivity of the hydrogel (Fig. 3d).[105] The above-mentioned mechanism provides inspiration for the preparation of ionic hydrogel-based gas sensors and humidity sensors for air quality detection. As another innovative chemical sensor, parallel electrode arrays can use the capacitance response to distinguish different liquid molecules (Fig. 3e and f).[106] The liquid to be detected forms a bridging electrode, which leads to an increase in the capacitance signal. The strength of the increasing capacitance is closely related to the polarity of the liquid molecules, while the duration of increasing capacitance is controlled by volatility and wettability. Consequently, different liquids can be identified according to the strength and duration of the increased capacitance.

3.2. Temperature sensors

The electrical signals of the hydrogel-based temperature sensors respond to changes of temperature. Changes of temperature would affect the migration rate of ions and the volume of temperature-sensitive hydrogels. Therefore, temperature sensors are mainly divided into two types: resistive temperature sensors based on the temperature–conductivity relationship and capacitive temperature sensors based on the temperature–volume relationship.[107]

The resistance of an ionic hydrogel is sensitive to temperature, as the increase in temperature would accelerate the migration of ions while favouring their dissociation.[108] Therefore, the resistance of a hydrogel decreases with increasing temperature. On this basis, the variations in temperature can be detected by measuring the resistance of a hydrogel (Fig. 4a).[109–111] Studies have shown that increasing the initial resistance of ionic hydrogels is beneficial to improve the temperature sensitivity.[112] Because the larger initial resistance means that the migration of ions faces greater barriers. At elevated temperatures, ions can overcome the obstacles of the network and move freely. Consequently, the effect of resistance reduction will be relatively more evident. On the other hand, the introduction of organic solvents with smaller specific heat capacity is also an effective strategy to enhance the temperature sensitivity of hydrogels.[112,113] When absorbing the same amount of heat, the hydrogel containing a solvent with a lower specific heat capacity has a higher temperature rise, resulting in more noticeable changes in resistance. For example, glycerin is introduced into the hydrogel by a solvent replacement method to improve temperature sensitivity.[112] Compared with hydrogels, the thermal sensitivity of glycerin organohydrogels has increased significantly from 2.95%/°C to 19.6%/°C. Notably, the organohydrogel temperature sensor exhibited an apparent response to the gentle touch of hot objects and non-contact sensation (Fig. 4b).

A capacitive temperature sensor is formed by sandwiching a piece of dielectric with two pieces of thermo-responsive hydrogel (Fig. 4c).[114] When the temperature reaches the critical temperature, the volumetric variations of the thermo-responsive hydrogels influence the distance of electrodes and contact area of hydrogels and a dielectric elastomer, thus altering the capacitance (Fig. 4d).

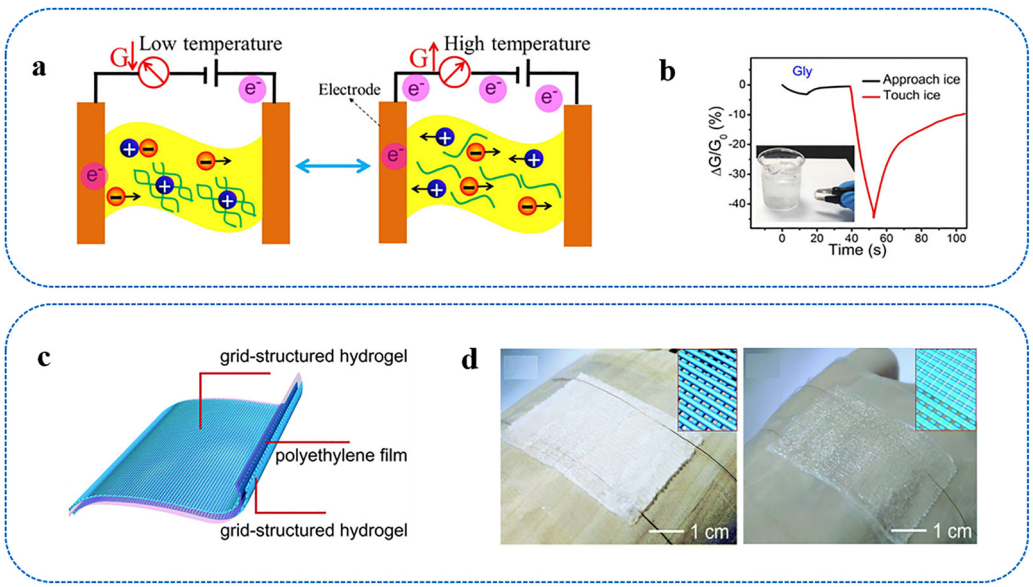

Fig. 4 Hydrogel ionic temperature sensors. (a) Schematic illustration of the working principle of a resistive temperature sensor. The increase in temperature facilitates improvements in the migration rate of ions and the dissociation of ions, thereby reducing resistance.[112] (b) Real-time response of the temperature sensor when approached and touched with ice water.[112] (c) Schematic diagram showing a capacitive temperature sensor based on a thermally responsive hydrogel electrode.[114] (d) When the critical temperature is reached, the capacitance of the sensor would increase due to the expansion of the hydrogel.[114]

3.3. Stress/strain sensors

Ion-conducting hydrogel-based stress/strain sensors convert mechanical stimuli into electrical signals. By monitoring the applied stress and strain, the operating state of the target can be judged to ensure its normal operation. From a theoretical perspective, such electromechanical responses originate from coupled ion transport and interfacial electrochemical processes. Specifically, the redistribution of mobile ions under deformation and applied electric fields can be described by the Poisson–Nernst–Planck (PNP) framework, which governs ion flux driven by concentration gradients and electric potential.[115] In addition, the formation of electrical double layers (EDLs) at hydrogel–electrode interfaces plays a dominant role in determining the effective capacitance and signal output.[116] According to the working mechanism, hydrogel stress/strain sensors can be divided into two categories: capacitance mode and resistance mode.[117]

A dielectric elastomer is sandwiched between two ion-conducting hydrogel layers to form a capacitive sensor. The capacitance of the EDL formed at the interface of a hydrogel and an electrode is much larger than that of a dielectric elastomer. Therefore, the equivalent circuit is close to the capacitance of the dielectric elastomer. The capacitance value is determined by $C = \varepsilon S/d$, in which ε, S and d are the permittivity, contact area, and thickness of the elastomer, respectively. If pressure is applied or the sensor is stretched, the thickness of the sensor decreases and the area increases, increasing the capacitance.[1] Thus, when the sensor deforms under an external force, stress and strain can be measured by the change in capacitance. The relationship between deformation and capacitance is predictable. When it is stretched by λ times, the original capacitance C_0 of the capacitive strain sensor and the capacitance after stretching C follow the linear relationship of $C = C_0\ \lambda$.[111]

For resistive sensors, a hydrogel can be regarded as a resistor, and varying the configuration of the polymer network and water molecules would cause changes in the resistance of the hydrogel (Fig. 5a), because the resistance of the hydrogel is $R = \rho l/A$,[118] which is determined by the resistivity (ρ) and geometry (cross-sectional area A, the length l). Deformation has a negligible effect on the ion conductivity of the hydrogel.[43,46] Therefore, the resistance of the hydrogel can respond to the deformation. By connecting the ion-conducting hydrogel to the resistance tester, stress and strain can be measured by testing the change in resistance. The change in resistance after deformation of a resistive sensor is also predictable: the resistance R scales as $R = R_0\lambda^2$ (R_0 is the initial resistance).[118] The performance of resistive sensors is mainly attributed to the properties of the hydrogel, so its relatively simple structure allows the advantages of the hydrogel to be directly demonstrated. For instance, the high stretchability of the hydrogel allows resistive sensors to measure large deformations and a self-healing hydrogel can effectively improve the durability of a sensor without being limited to the properties of other composite materials (Fig. 5b).[119] Some resistive sensors are capable of exhibiting bidirectional piezoresistive effects. For instance, a vitrimer heterogel (VHG) with bicontinuous structure demonstrates switchable hardness-gated ion transport pathways.[120] This behavior is closely associated with its two primary, mechanically tunable states, namely the stiff and soft states (Fig. 5c). A wide pressure response range and a tunable detection limit are critical for the performance of resistive sensors. For example, multiphase ionogels constructed by elastic ionogel frameworks and switchable poly(stearyl methacrylate) (PSMA) micro-inclusions exhibit pronounced stiffness-memory behavior.[92] As a result, resistive sensors derived from these ionogels demonstrate programmable pressure–response characteristics and wide pressure range (Fig. 5d), making them well suited for operation across diverse application scenarios.

Conducting resistance detection on a piece of hydrogel in a classic structure of a parallel-plate capacitive sensor can achieve simultaneous detection of capacitance and resistance (Fig. 5e). The capacitance sensor is only sensitive to deformation, but the resistive sensor is sensitive to temperature and deformation at the same time, so a sensor system that can sense multiple stimuli is constructed (Fig. 5f and g).[111]

Resistive sensors typically exhibit higher sensitivity owing to the strong dependence of electrical resistance on ion mobility and the deformation of conductive pathways within the hydrogel network.[121] However, this mechanism also makes them more susceptible to environmental factors such as temperature, humidity, and ion concentration, leading to signal cross-sensitivity and reduced stability.[122]

In contrast, capacitive sensors primarily rely on changes in geometric configuration and dielectric properties, making their signal output less sensitive to fluctuations in ionic transport. This inherent decoupling from ion mobility variations contributes to improved signal stability and reproducibility, particularly in complex or dynamic environments.[123] Nevertheless, their sensitivity is typically lower, particularly under small deformations, due to the relatively weak dependence of capacitance on structural changes.

From a materials design perspective, resistive sensors typically require highly conductive and deformable ionic networks to maximize sensitivity, whereas capacitive sensors depend on mechanically robust dielectric layers and well-defined interfacial structures to ensure a stable signal output.[124] Consequently, the choice between resistive and capacitive sensing mechanisms involves an inherent trade-off between sensitivity and signal stability, which should be carefully optimized according to specific application requirements.[122]

3.4. Touch sensors

Hydrogel-based touch sensors are used to detect physical contact, and they can determine the occurrence, location, and even proximity of objects. The sensing mechanism can be further understood from an interfacial electrochemical perspective. Mechanical stimuli induce spatial redistribution of ions and modulation of the electrical double layer structure, which directly affects interfacial capacitance and impedance.[125] Such processes are governed by ion transport dynamics and

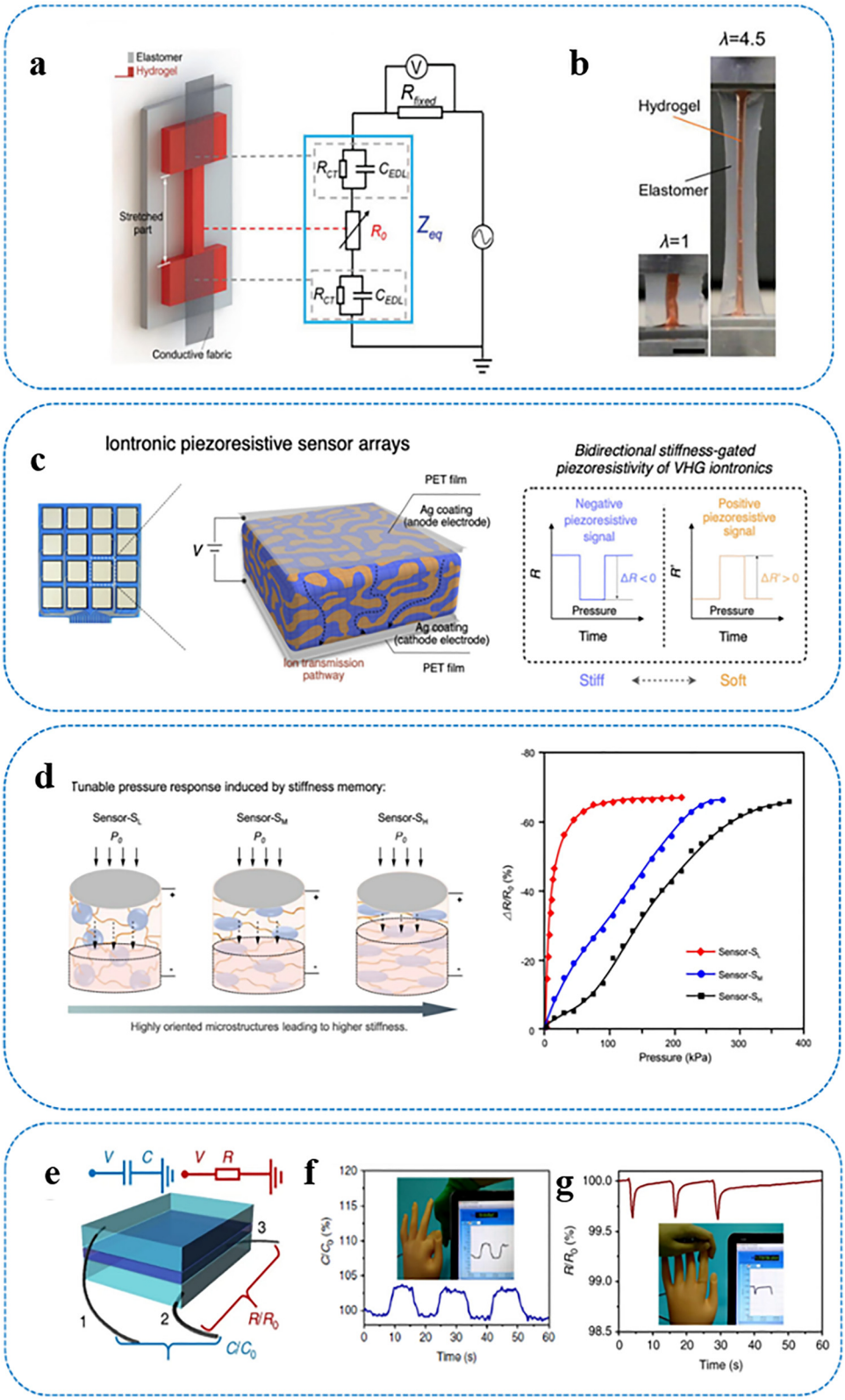

Fig. 5 Hydrogel-based ionic stress/strain sensors. (a) Schematic of a resistive stress/strain sensor. The resistance of the hydrogel increases with stretching.[118] (b) A resistive stress/strain sensor can withstand large deformations.[118] (c) Schematic diagram of VHG iontronic piezoresistive sensor arrays with bidirectional stiffness-gated piezoresistivity capabilities.[120] (d) Schematic diagram showing the pressure-response change with varied stiffness of the heterophasic ionogels.[92] (e) Schematic diagram of a sensor that monitors both capacitance and resistance.[111] (f) The capacitive signals respond to changes in strain. For example, when a sensor monitors the bending of a finger.[111] (g) The resistive signals respond to changes in temperature when a finger touches the sensor.[111]

interfacial charge screening effects, highlighting that the sensing behavior is intrinsically controlled by electrochemical–mechanical coupling rather than purely geometric deformation.[126] Based on ionic hydrogels, next-generation stretchable and biocompatible touch sensors can be developed. This system can easily and intuitively realize human–machine interaction by combining a hydrogel touch sensor and a display. Hydrogel-based touch sensors can be divided into two categories: capacitive sensing and electrostatic induction sensing systems.[127]

A touch sensor adopts a surface capacitive system, in which the same voltage is applied to all corners.[128] When a grounded conductor touches the surface of the hydrogel, a potential difference is generated between the electrode and the touch point (Fig. 6a). Current is generated between the electrode and the grounded conductor. The closer to the contact point, the current will be greater. The location of the touch point is determined by comparing the magnitude of the current. Thanks to the high stretchability, high transparency and low modulus of hydrogels, touch sensors can be comfortably

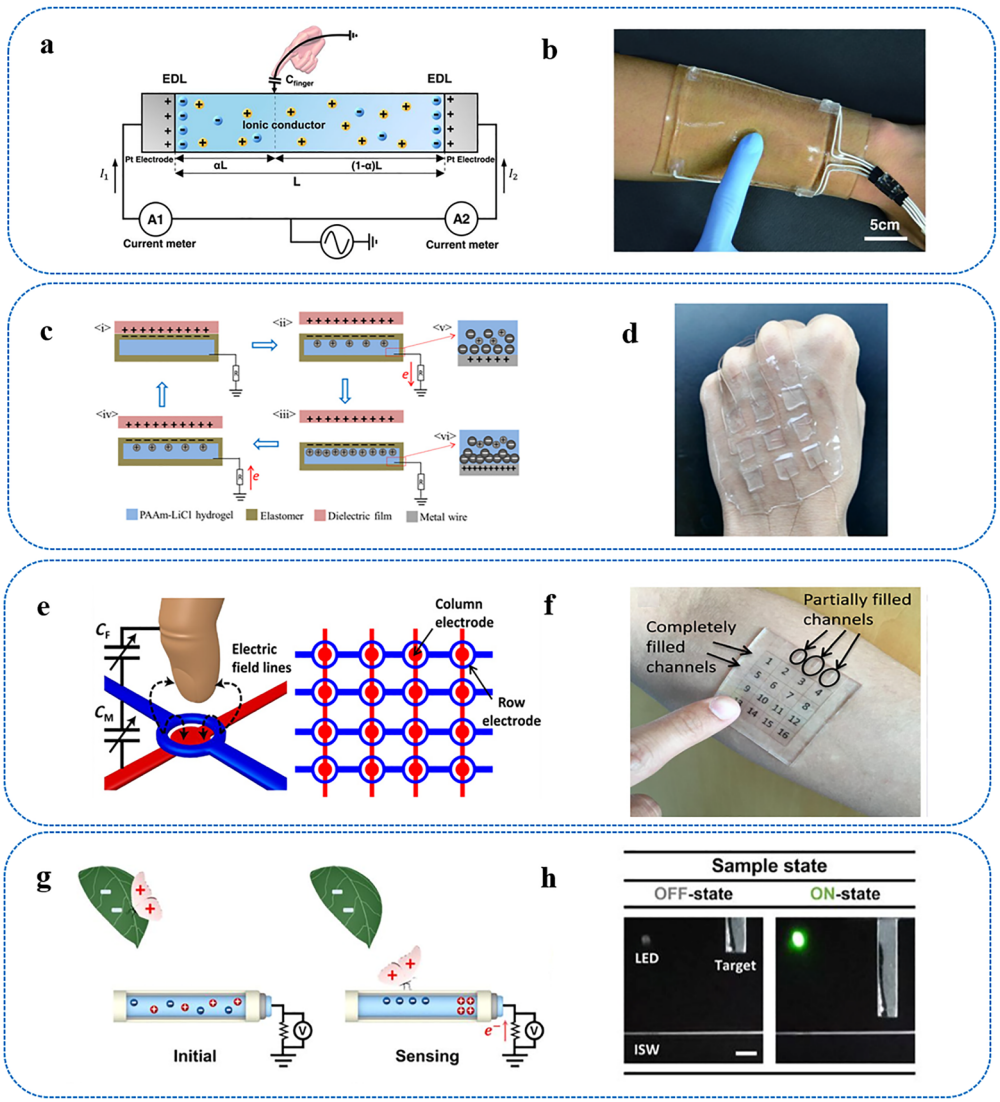

Fig. 6 Hydrogel-based ionic touch sensors. (a) Schematic diagram showing a surface-capacitive touch sensor. The touched position of the ground conductor is confirmed by the current caused by the potential difference between the touch point and the electrode.[128] (b) The ionic touch sensor was attached to an arm for operation.[128] (c) Schematic diagram showing the working mechanism of a triboelectric touch sensor. When an object touches the sensor, contact electrification occurs at the interface. Detaching and attaching of a charged object induces voltage across the external load by electrostatic induction.[94] (d) Schematic diagram of a triboelectric touch sensor with 9 pixels attached on a hand.[94] (e) Schematic diagram showing a capacitive proximity sensor. The coupling disc-shaped and ring-shaped electrodes generate a vertical electric field to detect approaching objects.[136] (f) The transparent sensor array combined with a printed number pad is attached to the arm.[136] (g) Schematic illustration of the working principle of a proximity sensor based on electrostatic induction. When an object approaches the sensor, the sensor will generate electrostatic induction to detect the object.[137] (h) Using a pre-programmed circuit, a LED is turned on when the induced voltage generated by the approaching object reaches the threshold.[137]

attached to the human body to provide a visual man–machine interface (Fig. 6b). The touch sensor is further endowed with pressure-sensitive adhesiveness and self-healing properties to improve the practical performance *via* an innovative hydrogel.[129,130]

Triboelectric nanogenerators (TENGs) rely on the coupling effect of contact electrification and electrostatic induction to convert mechanical motion into changes of electrical signals.[131,132] TENGs usually have four working modes, namely the contact-separation mode, sliding mode, freestanding mode, and single electrode mode.[133,134] The recently developed TENG based on an ion-conducting hydrogel has natural flexibility, high transparency and high stretchability, which is a breakthrough for energy harvesters with fixed shapes.[94] The hydrogel-based TENG adopts a single-electrode mode, in which the elastomer and hydrogel serve as the electrification layer and electrode. The hydrogel electrode is encapsulated in an elastomer dielectric cell and connected to an external load by metal. As we all know, when two objects touch, electron transfer would occur at the interface. But due to the coincidence of the interface, the two objects show electrical neutrality. When the interface is separated, the two objects are charged with an equal amount of opposite charges due to the redistribution of electrons. This contact charging phenomenon would exist in the insulator for a relatively long time, thus generating static electricity. When the dielectric makes contact with the TENG's elastomer, electrons are transferred. When the dielectric leaves the elastomer, the static charges can induce the oppositely charged ions in the hydrogel to accumulate at the interface to balance the static charges. At the same time, an EDL is formed at the metal/hydrogel interface. Electrons flowing from the metal wire to the ground would form a current until all the static charges in the elastomer are screened. If the moving dielectric returns to the elastomeric state, a current in the opposite direction is generated. By repeating this process, an alternating current will be generated (Fig. 6c). Sensors based on electrostatic induction do not require an external power source, which is conducive to its application in mobile devices (Fig. 6d).

Humans obtain the tactile sensation by detecting changes in friction, roughness, hardness, and temperature.[135] In contrast, the hydrogel-based touch sensors rely on capacitive and electrostatic induction, so it exhibits a proximity-sensing function that surpasses the human body's own tactile sensation. In order to sense the proximity of an object, a capacitive touch sensor is assembled using an ionic hydrogel-based electrode array containing disc-shaped and ring-shaped electrodes separated by elastomers.[136] The coupling of the two electrodes generates a vertical electric field. A nearby object can reduce the coupling between the electrodes and be induced. The hydrogel electrodes enable the sensor to detect touch during bending and stretch, and can detect the position of multiple objects (Fig. 6e and f). Similar to the phenomenon of contact electrification, objects close to the sensor can also cause electrostatic induction to generate induced currents to monitor the presence of objects (Fig. 6g and h).[137]

For hydrogel-based touch sensors, maintaining high signal fidelity is particularly challenging due to their strong coupling with external environments and complex stimuli. Ionic hydrogel systems are inherently sensitive to ambient humidity, which can significantly alter their electrical properties and cause pronounced signal drift and instability in sensing outputs.[138] Moreover, variations in contact conditions, such as pressure distribution and electrode–hydrogel interface fluctuations, can introduce additional noise and reduce the accuracy of spatial or proximity sensing, as these factors dynamically modulate interfacial impedance and effective contact area, thereby generating signal artefacts and degrading signal-to-noise ratio.[139] In high-density sensor arrays, undesired signal interference and crosstalk between adjacent sensing units further degrade signal clarity, posing challenges for precise touch localization. Additionally, the capacitive nature of ionic systems can amplify low-frequency noise and slow response dynamics, limiting their ability to faithfully capture rapid or subtle touch events. Consequently, strategies to decouple environmental effects, stabilize interfaces, and suppress signal interference are crucial for advancing high-fidelity ionic touch sensing systems.[140]

4. Hydrogel ionic transporters

Humans coordinate the functions of sensing, deciding, and acting in different parts through long-distance and rapid ion transport in nerve fibers. Hydrogel ionic sensory systems rely on ion transporters to realize the interconnection of ionic sensors, ionic processors, and ionic effectors. An ion transporter is a connection element based on ion conduction. It is not only the link among the components of ionic sensory systems, but also the interface between electronic and biological systems.

4.1. Ionic cables

Hydrogel ionic cables enable transport signals over long distances and at high speeds.

An ion cable based on an electric double layer mimics the function of an axon, which consists of two layers of hydrogel separated by a layer of elastomer (Fig. 7a).[141] Based on the advantages of the structure, the migration of ions in the ionic cable only occurs locally and does not require passing through the two electrodes. An increase of 16 orders of magnitude in ionic diffusivity enables the ionic cable to transmit an action potential of stable amplitude at a speed over 100 m s^{-1}, and can transport a signal up to 100 MHz within 10 cm (Fig. 7b). It is worth noting that, due to the limitation of the electrochemical window of the hydrogel, the ionic cable can only be applied under an AC voltage with an amplitude within 1 V. The ion conductive hydrogel provides high transparency to the ionic cable, while allowing it to function normally when stretched more than eight times. Proportionally reducing the device size will not affect the performance of the ionic cable. These interesting properties pave the way for stretchable ion propagation technology and its miniaturization.

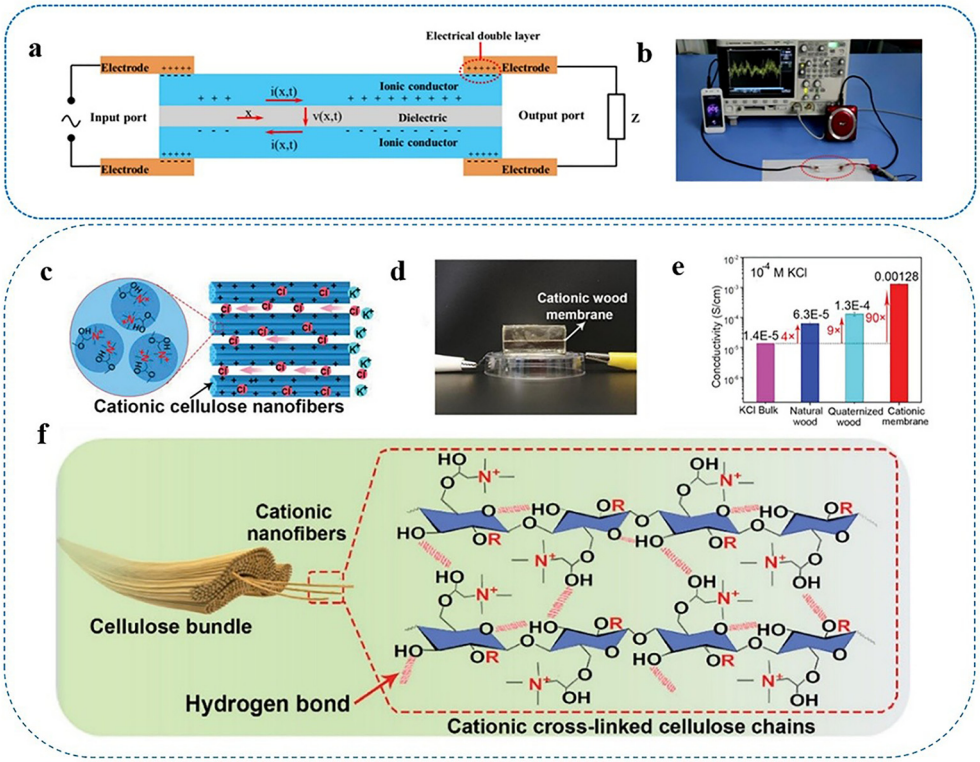

Fig. 7 Hydrogel-based ionic cables. (a) Schematic diagram of the working mechanism of ionic cables. Ions migrate locally in the cable without crossing two electrodes.[141] (b) Ion cables were used to transport cell phone signals to speakers and oscilloscopes.[141] (c) Rapid and selective migration of ions in the densified hydrogel cable with nanochannels.[148] (d) Device diagram for testing the ion conductivity of the hydrogel cable with nanochannels.[148] (e) The densified hydrogel cable with nanochannels has a significantly improved conductivity.[148] (f) Schematic of the hydrogen bonding among the molecular chains of the cationic wood membrane.[148]

Signal transduction in organisms involves ion transport through nanochannels.[142–145] Studies have shown that ion transport in a charged channel with a size equivalent to the Debye length exhibits a different nanofluidic transport behavior from the whole.[146] In order to simulate the ion migration behavior of biological systems, densified natural materials with surface charges are used to obtain a hydrogel ionic cable with nanochannels for ion transport.[147–151] The densified narrow nanochannels are conducive to the rapid migration of ions. On the other hand, the charges on the surface of the nanochannels facilitate the enrichment of the conductive ions, thus showing an increase in ion concentration (Fig. 7c). At low ion concentrations, the hydrogel ionic cable with nanochannels exhibits conductivity that is 90 times higher than that of bulk solutions (Fig. 7e).[148]

4.2. Ionic interfaces

An ionic interface is used for ion transport between electronic systems and biological systems. At the fundamental level, ionic–electronic interfaces are governed by interfacial electrochemical physics. When an ionic conductor contacts an electronic conductor, mobile ions accumulate near the interface to form electrical double layers, which act as nanometer-scale capacitors and dominate charge transfer behavior. The structure and dynamics of these EDLs, together with ion migration in the bulk electrolyte, can be described using continuum ion transport theories such as the Poisson–Nernst–Planck model.[115,116] Utilizing an ionic interface can record various bioelectronic signals, and stimulate the biological systems simultaneously. On the other hand, ionic interfaces provide a reliable and safe connection mechanism that helps patients with sensory dysfunction integrate artificial organs into the human body. Thus, ionic interface technology realizes bidirectional communication between machines and living beings.

Commercial wearable and implantable electronic devices can collect and transmit biological signals in different parts of the human body and apply them to clinical diagnosis and treatment, which has achieved great success.[152,153] However, conventional electronic devices rely on rigid metal materials that are severely mismatched with the physical and mechanical properties of human tissue. Therefore, they are prone to high interface impedance due to loose contact when used *in vitro*;[154,155] when they are implanted, cells will wrap the interface and block the signal[156] and even produce an inflammatory response.[157] At the same time, because electronic equipment and the human body have different signal carriers, the threshold voltage required for the conversion of electrons to ionic current at the biological interface often causes pain and damage to biological tissues.[158,159] Due to the inherent biocompatibility, the modulus that matches the human tissue, and

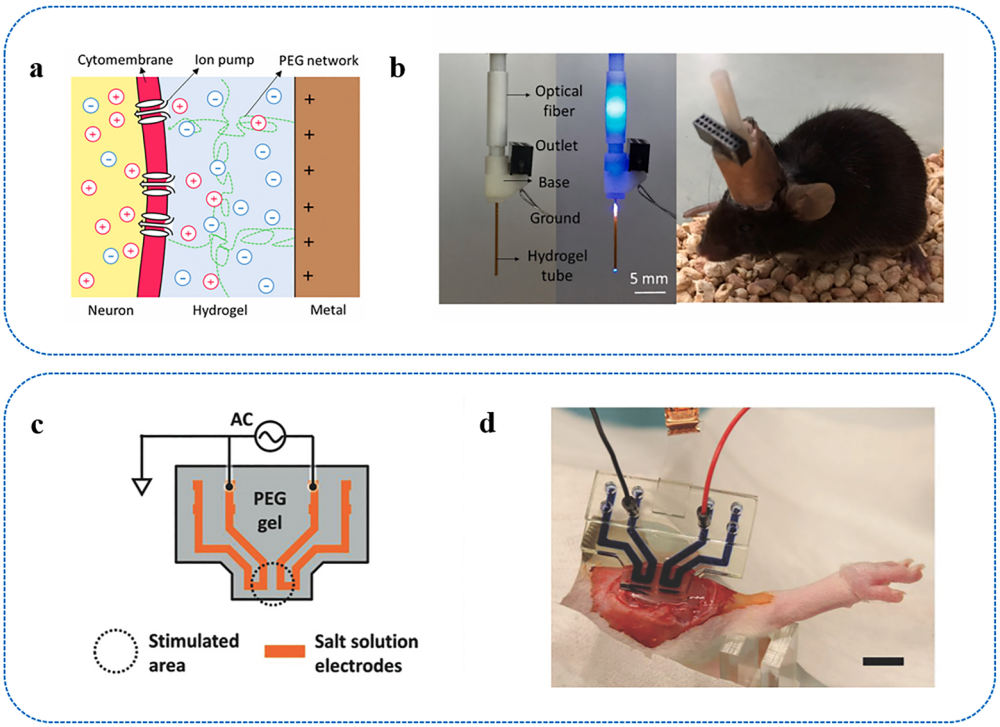

Fig. 8 Hydrogel-based ionic interfaces. (a) Schematic diagram showing the working principle of the hydrogel neuroelectronic interface. Ions are transported between the organism and the electrode through the hydrogel neural interface.[165] (b) A hydrogel neural interface was implanted in a mouse for applying laser stimulations and detecting.[165] (c) Schematic diagram of the ionic interfaces of ATPS. The PEG hydrogel acts as a shell to prevent the ionic solution contained in it from spreading.[158] (d) An ionic interface of ATPS was placed on the muscle for electrical stimulation.[158]

the ideal ionic conductivity, ionic hydrogels effectively eliminate the problems of current conversion and mechanical mismatch between the electrode and the tissue.[31,160] Hence, they have been widely used in non-invasive applications, such as wearable devices and epidermal electrodes.[161–163] However, ionic hydrogels can exchange substances with the internal tissue media of the human body (*e.g.*, ion leakage caused by differences in ion concentration), which limits their application in invasive devices.[158,164]

Recently, the signal monitoring and stimulation of the mouse brain has been achieved *via* an ion-conducting hydrogel encapsulated by an elastomer (Fig. 8a).[165] The hydrogel contains artificial cerebrospinal fluid (ACSF), which helps the hydrogel to simulate the living environment of neurons chemically, mechanically, and electrically to reduce rejection. The frozen elastomer-sealed hydrogel interface can be easily inserted into the brain of a mouse and collect nerve signals after thawing. Thanks to the high light transmittance of the hydrogel, a single fiber of the hydrogel can simultaneously perform optical stimulation (Fig. 8b). Neuro-compatible hydrogel interfaces have great potential in clinical applications.

On the other hand, the aqueous two-phase system (ATPS) composed of a polyethylene glycol hydrogel and salt solution can improve the stability of ions *in vivo*.[158] A polyethylene glycol hydrogel can provide a flexible conductive shell in direct contact with tissues, and the separated salt solution contained in the hydrogel provides high ionic conductivity without ion diffusion into the surrounding tissue media (Fig. 8c). When a voltage is applied, the induced ionic current will be transmitted in the channel perfused by the salt solution, and can be transferred to the electrical response component *via* the polyethylene glycol hydrogel. In long-term applications, the hydrogel of aqueous two-phase systems enables effective electrical stimulation of muscles (Fig. 8d).

A key challenge for practical applications lies in the integration of ionic devices with conventional CMOS-based electronic systems. While ionic interfaces have demonstrated excellent performance in bridging biological systems and electronic devices, extending these concepts to standardized electronic platforms remains nontrivial. Unlike electronic circuits that rely on electron transport, ionic systems operate through ion migration,[166] resulting in fundamental mismatches in signal carriers, operating voltages, and response times. These differences originate from the intrinsically slower dynamics of ion transport and the electrochemical nature of ionic conduction, which can be described by coupled ion transport and interfacial models.[167] Consequently, efficient ion-to-electron signal transduction and seamless interfacing with CMOS circuits remain challenging, limiting the development of fully integrated ionotronic systems.

5. Hydrogel ionic processors

Biological processors exhibit a highly dynamic structure and a non-linear operation mode. Synapses in neuronal networks

continuously change formation and stability in response to stimuli and the migration of ions also shows the characteristics of precise adjustment.[168] Compared to machines that can only respond to programmed stimuli, biological decision-making systems allows organisms to dynamically adapt to changes in the environment and make more intelligent decisions. Based on hydrogels to achieve precise ion migration, it is expected to develop smart ionic processors that can be used in modern science and technology. Hydrogel-based ionic processors are mainly divided into three categories, diodes for rectifying ionic signals, transistors for adjusting and amplifying ionic signals, and memristors for storing ionic signals (Table 2).

5.1. Ionic diodes

Hydrogel ionic diodes can be formed by two pieces of hydrogels containing polyanions and polycations respectively. Ion diodes have obvious rectification performance: under forward bias, polyelectrolyte counter ions move across the interface, thereby forming a conduction current. Under reverse bias, counter ions move to the nearby electrode and cannot pass through the interface to form a current. Hydrogel ionic diode membranes exhibit current density and rectification ratios comparable to or higher than organic-based diodes.[175] Nanopores with surface charge have been applied to ion rectification (Fig. 9a).[176,177] It has been reported that nanopores modified by stimuli-responsive DNA hydrogels can achieve high ion flux and adjustable rectification ratios.[169,178] DNA hydrogels are assembled to the tip of the conical nanopore. Hydrophilic networks of the hydrogel and introduced negative charges effectively contribute to the transport of cations. The adjustable stiffness state and pH stimulation of DNA hydrogels can precisely control the gated states of on/off and the transport direction of cations or anions (Fig. 9b).

Miniaturized ion diodes and transistors are essential for complex integrated circuits and fast response to external inputs.[175,179] By irradiating ultraviolet light on the patterned mask, researchers can polymerize polymers at the target position in the microfluidic channel (Fig. 9c).[180] This is widely used in microfluidic devices based on charge-selective polymers. Based on this technology, a polyelectrolyte hydrogel diode was prepared on the microchip channels of hundreds of micrometers, and the diode showed significant rectification (Fig. 9d).[175] Integrating multiple hydrogel diodes on a microchip will produce ionic logic gates including AND, OR and NAND. The fluorescent emission on the polyelectrolyte plug visually displays input signals. These studies are valuable explorations of ion diodes in the field of bionic integrated circuits allowing the functional control and real-time display of ionic current. Ionic signal amplification have realized through an open-junction ionic diode and the mechanism of ion-to-ion signal amplification was proposed.[181,182] At the open junction of the depletion region, an ion solution is injected to temporarily neutralize the depletion region. A breakdown current will generate with a significant increase in signal strength.

Stretchable ionic diodes have been investigated as well.[170,183,184] The polyelectrolyte hydrogel is modified by utilizing methacrylate to prepare a stretchable ionic diode, which exhibits rectification behavior beyond the stretch of 3, and maintained its performance under repeated deformation (Fig. 9e).[183] Studies have shown that increasing the stretching ratio has a weakening effect on the rectification ratio, which is because of the increasing effect of stretching on the resistance of the hydrogel (Fig. 9f).[170] Stretchable ion diodes can find potential applications in stretchable ion circuit systems and flexible wearable devices.

Despite the promising rectification behavior of hydrogel ionic diodes, their practical application faces significant challenges. One critical issue is the temporal stability of rectification performance under sustained bias. Ionic rectification fundamentally arises from asymmetric ion transport and the formation of ion enrichment and depletion regions at heterojunction interfaces under opposite bias conditions.[185,186] Continuous ion migration under prolonged bias may lead to persistent concentration polarization, structural rearrangement of the hydrogel network, and potential dehydration effects, all of which can degrade the rectification ratio over time.

In addition, the relatively slow ion dynamics, governed by diffusion and migration processes, fundamentally limit the response speed of ionic diodes compared to electron-based devices.[185] Therefore, the design of ionic diodes requires balancing rectification performance, response speed, and long-term stability, which remains a key challenge for their integration into complex iontronic circuits.

Recent studies have demonstrated that ferroelectric nanochannels with spontaneous polarization enable field-free unidirectional ion transport, offering a stable rectification

Table 2 Comparison of the performance of different hydrogel ionic processors

Type	Commutating ratio	Operating voltage range	Maximum current	Ref.
Ionic diodes				
DNA hydrogel nanochannel	52.75	−2–2 V	30 nA	Wu *et al.*[169]
Stretchable hydrogel diode	18.5	−7.5–7.5 V	3 mA	Wang *et al.*[170]
Ionic transistors				
NPN ion bipolar junction transistor	35	30	Rise time: 9 s/fall time: 3 s	Tybrandt *et al.*[171]
PNP ion bipolar junction transistor	39	100	Rise time: 12 s/fall time: 5 s	Tybrandt *et al.*[172]
Ionic memristors				
Bipolar polyelectrolyte gel memristor	8	4000 s	0.7 μA	Zhang *et al.*[173]
All-soft-matter liquid metal memristor	100	3 h	3 μA	Koo *et al.*[174]

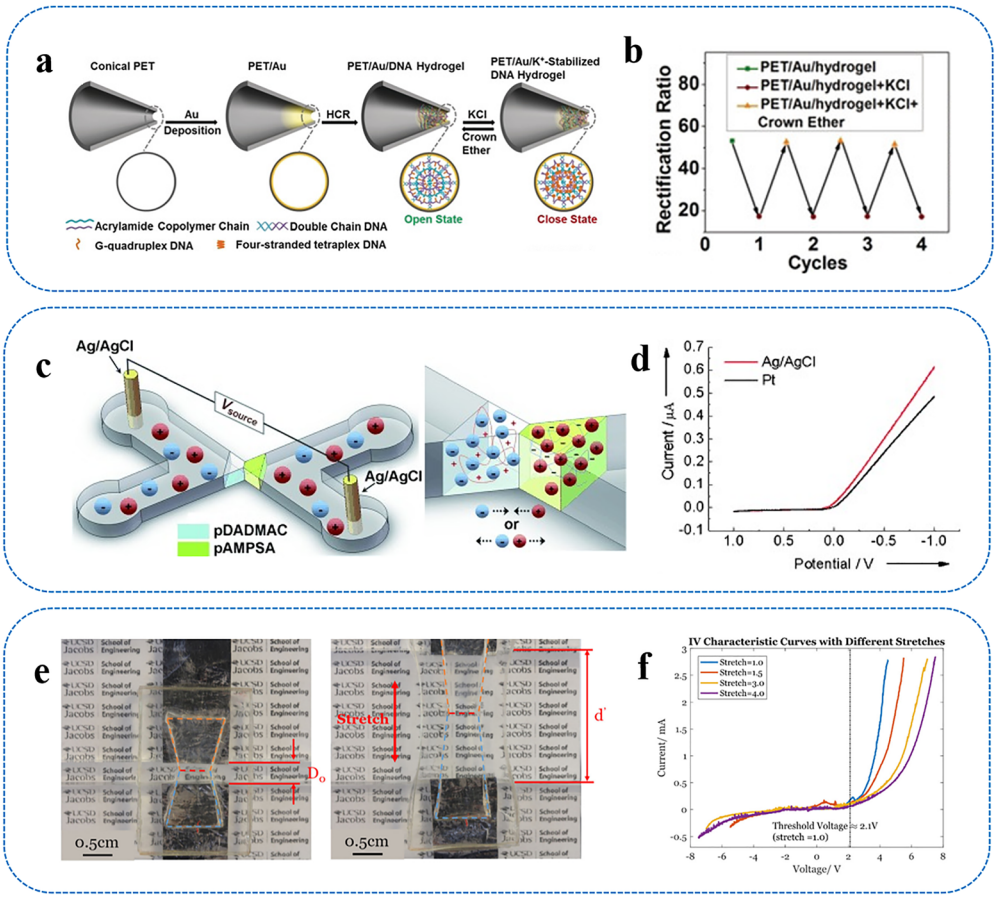

Fig. 9 Hydrogel ionic diodes. (a) Illustration of the preparation process of the Hydrogel-based conical nanochannel ionic diode. The nanochannel ionic diode can reversibly switch the rectification ratios.[169] (b) Schematic illustration of a polyelectrolyte hydrogel ionic diode in a microchip.[169] (c) A hydrogel ion diode enabling selective ionic currents.[175] (d) Schematic illustration of a stretchable hydrogel ionic diode.[175] (e) The rectification ratio of an ionic diode decreases slightly with stretching.[170] (f) IV characteristic curves with different stretches.[170]

platform for low-power ionic circuits. For instance, ionic diodes employing ferroelectric $BiFeO_3$ (BFO) nanopore membranes maintain stable operation for 50 minutes under alternating ±1 V bias without observable decay in ionic current.[187]

5.2. Ionic transistors

Field effect transistors based on polyelectrolyte hydrogels can also be prepared by using pattern masking photopolymerization.[188] A polycationic hydrogel and a polyanionic hydrogel are formed at two positions on the microchip (Fig. 10a), allowing the selective passage of anions and cations, respectively. Under the action of the gate voltage, the polyelectrolyte plug extracts ions, resulting in the formation of an ion depletion region and a decrease in source–drain current (Fig. 10b). The pnp and npn-type ion bipolar junction transistors (IBJTs) can be used to construct functional elements similar to CMOS

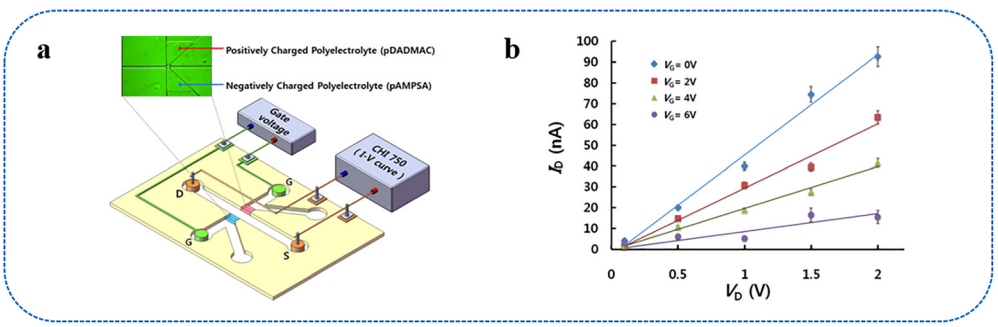

Fig. 10 Hydrogel ionic field-effect transistor. (a) Schematic illustration of a field-effect transistor in a microchip. By applying the gate voltage, a field-effect transistor induces the main channel connected to source and drain electrodes.[188] (b) Output characteristics of a polyelectrolyte junction field effect transistor (pJFET).[188]

to deliver appropriate signal amplification and logical gate functions.[171,172]

However, this ion-based gating mechanism inherently relies on ion migration and diffusion processes, which are significantly slower than electron transport and thus limit the response speed of ionic transistors.[189] In addition, the formation and relaxation of ion depletion/enrichment regions require finite diffusion times, leading to delayed switching and hysteresis effects.[190] Furthermore, while ion accumulation at interfaces can provide high capacitance and efficient gating, it may also induce structural or compositional changes in the active layer, affecting device stability and reproducibility.[191] Therefore, the design of ionic transistors involves balancing gating efficiency, response speed, and operational stability.

5.3. Ionic memristors

A memristor is a nonvolatile device whose resistive state changes based on the history of current or voltage passing through it, allowing it to retain memory without power.[192,193] Taking advantage of low energy consumption, high data density, and self-adaptation, memristors may become the core of next-generation storage and computing devices.[173,194] A hydrogel-based memristor consists of two liquid metal (EGaIn) electrodes wrapped and separated by two hydrogels with different pH (Fig. 11a).[174] The forward bias causes the liquid metal to form an insulating oxide layer (Ga_2O_3) to inhibit ion current, while the reverse bias can eliminate the metal oxide layer to achieve conduction of current (Fig. 11b). It is similar to the accumulation and extrusion of Ca^{2+} in the synapses. The oxidation and reduction state of the liquid metal depends on the applied electrical bias and the pH of its local environment. Memristors based on ion-conductive hydrogels can achieve effective resistance switching and remember the final state. A memristor is a continuously tunable intelligent device like a synapse. It can adaptively change its performance, suggesting the possibility of developing intelligent memory and thinking. The favorable biocompatibility of hydrogels makes these devices promising for bionic systems, such as artificial brain-mimicking or neuromorphic structures.

6. Hydrogel ionic effectors

Hydrogel ionic effectors are located at the end of the sensory system and is an element used to feedback and express the processed information. At present, hydrogel effectors are mainly divided into actuators expressed in a mechanical form and optoelectronic devices expressed based on optical signals.

6.1. Ionic actuators

The first type of ionic actuators is based on electrostatic force. The hydrogel actuators can turn the input voltage into mechanical motion. The structure of an actuator is the same as that of a capacitive sensor, including a dielectric elastomer layer sandwiched between two ion-conducting hydrogels (Fig. 12a). When a high voltage is applied between the hydrogels, the anions and cations in the hydrogels move directionally, forming ionic accumulation layers of opposite charge along each hydrogel/elastomeric interface. The attractive force of opposite charges between the hydrogels would squeeze the elastomer layer (Fig. 12b).[43] The capacitance of the interface between the electric double layer and the dielectric elasticity is very different. In order to meet the charge balance, even if the applied voltage exceeds 1 kV, the interface voltage between the hydrogel and the metal remains less than 1 V, so that they will not undergo electrochemical reactions. The actuators based on ion-conducting hydrogels have the advantages of high deformability (fracture stretch 4.6 ± 0.3), fast response ($\tau_{inertia} \approx 1 \times 10^{-3}$ s), lightweight, and high transparency (96.95% average transmittance),[195] which can be applied to various forms of feedback expression, such as artificial muscles and fast-moving soft robots that provide feedback through actions (Fig. 12c),[43,196,197] surface texture change devices for tactile feedback through local deformation (Fig. 12d),[135] and speakers that express acoustical signals through mechanical vibration (Fig. 12e).[43]

The second type of ionic actuators is based on the difference in the motion state of the counterion and polymer chains in the polyelectrolyte hydrogel under the action of an electric field.[198–200] When an external electric field is applied to the

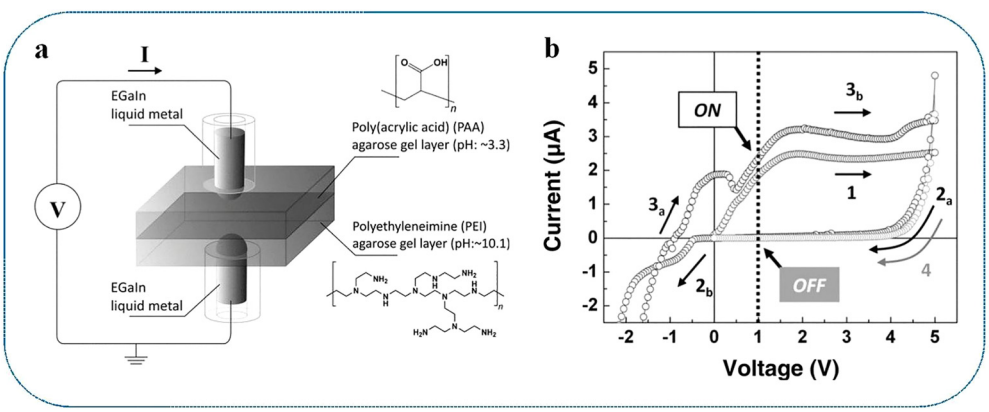

Fig. 11 Hydrogel ionic memristors. (a) An ionic memristor consists of liquid metal electrodes and hydrogel electrolytes with different pH.[174] (b) The characteristic curve shows the rectification performance of an ionic memristor.[174]

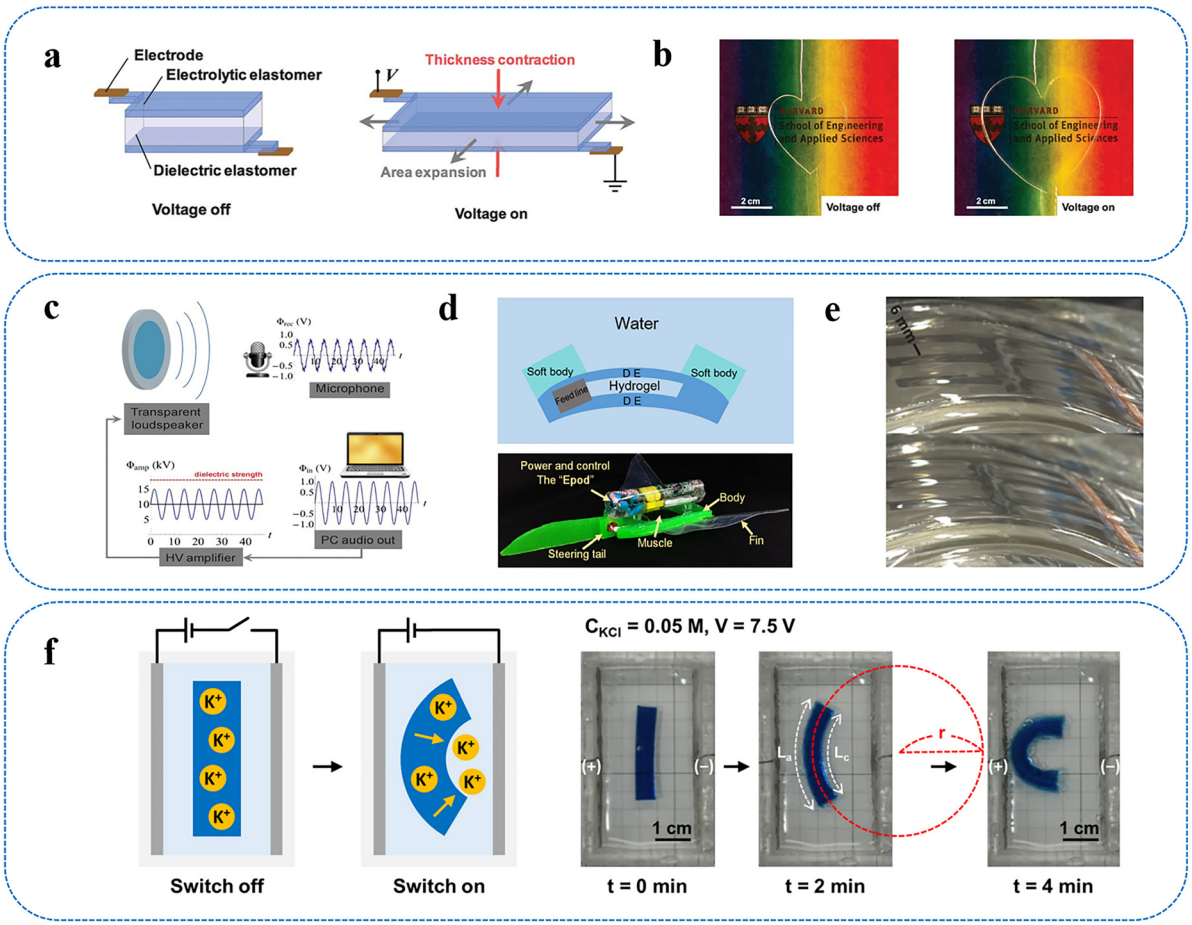

Fig. 12 Hydrogel-based ionic actuators. (a) Schematic illustration of the working principle of an ionic actuator is based on electrostatic force. The application of voltage causes the hydrogel layers on both sides of the elastomer to produce accumulation layers of opposite charges at the interface, thereby squeezing the elastomer.[43] (b) The actuator can produce a large deformation.[43] (c)–(e) Application of actuators: (c) speaker;[43] (d) fast-moving soft robots;[196] (e) surface texture change device for tactile feedback.[135] (f) Schematic diagram showing the working mechanism of an ionic actuator based on the difference in the motion state of the counterion and polymer chains. When an electric field is applied to the polyelectrolyte hydrogel, the osmotic pressure generated by the movement of counter ions to the electrode bends the hydrogel.[199]

polyelectrolyte hydrogel, only the counterions moving toward the electrode carry water away from the hydrogel through hydration.[198] This causes anisotropic shrinkage of the hydrogel accompanied by water extrusion. When the polyelectrolyte hydrogel is placed in an aqueous solution, the counterions and the ions in the aqueous medium with opposite charges to the counterions migrate in contrary directions, respectively. The osmotic pressure brought by the ion gradient caused the asymmetric swelling of the hydrogel (Fig. 12f).[199]

6.2. Ionic optoelectronic devices

The hydrogel optical effectors can visually express and feedback information through changes in color and transmittance under electrical stimulation. The ion-conducting hydrogels with high transparency and high refractive index is the guarantee for realizing the efficient change of optical information.[49,201,202] The research on ionic hydrogel optical communication devices mainly involves three types: electrochromic, capacitive optoelectronic, and electro-zoom devices.

Electrochromic devices have the advantages of high contrast and low driving voltage.[203] Electrochromic materials including inorganic materials (such as transition metal oxides) and organic materials (such as conjugated polymers), can change their color and transmittance through a reversible oxidation–reduction reaction caused by voltage application.[204] With its high transparency and compatibility, a hydrogel can be used simultaneously as a transparent electrode, electrolyte and electrochromic material storage layer, greatly simplifying the device structure to improve performance and reduce manufacturing costs (Fig. 13a). The hydrogel-based electrochromic device with a three-layer structure can obtain evident transmittance modulation and high coloring efficiency at a lower driving voltage (about 1 V) (Fig. 13b).

In a capacitive optoelectronic device, a layer of electroluminescent material (*e.g.*, liquid crystal[205] and phosphor[46,206]) is sandwiched between two ionic hydrogels and two elastomer layers (Fig. 13c). When an AC voltage is applied, the hydrogel acts as an ionic conductor to project an electric field to the

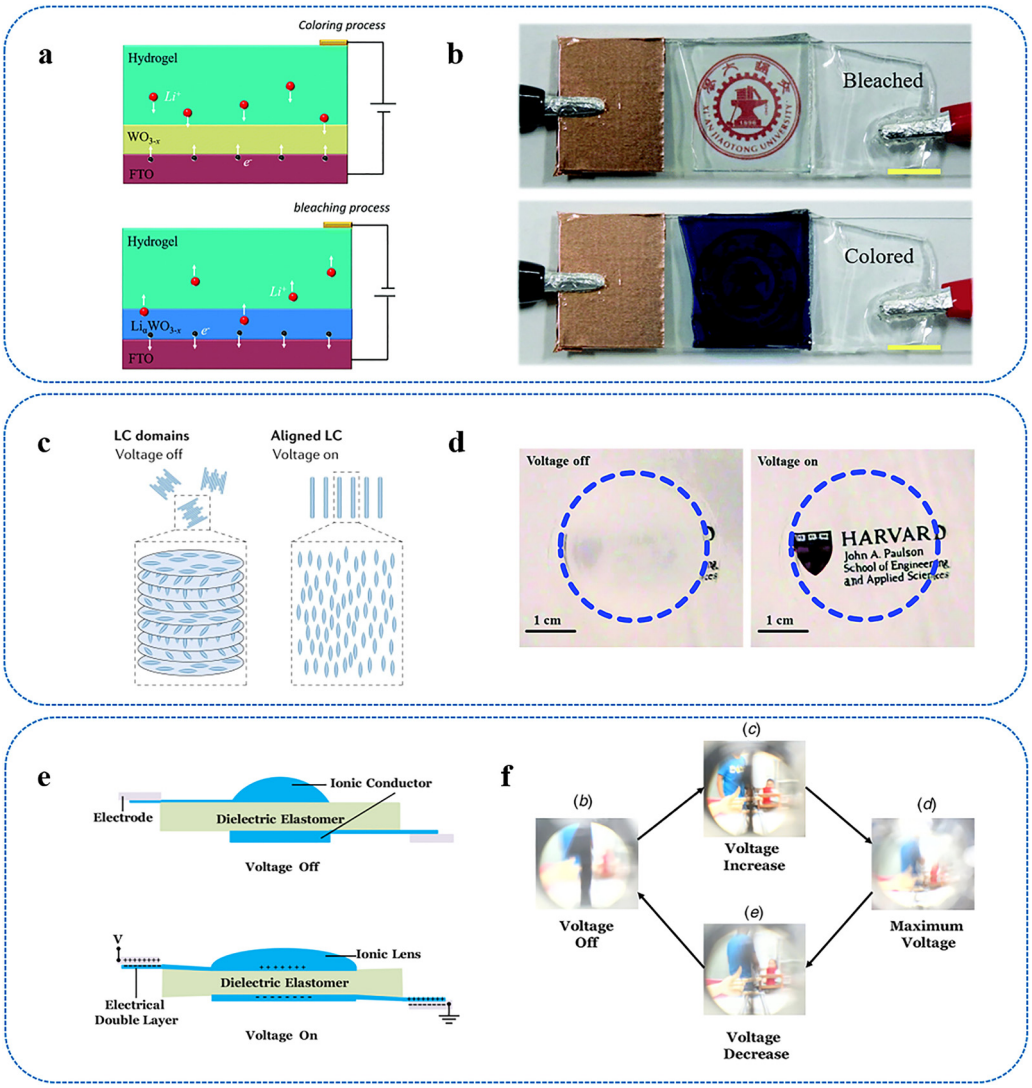

Fig. 13 Hydrogel-based ionic optoelectronic devices. (a) Schematic illustration of the working mechanism of the electrochromic device.[204] (b) The transmittance and color of the hydrogel can be effectively adjusted by applying voltage.[204] (c) Schematic illustration of the working principle of a capacitive liquid-crystal device. The arrangement direction of the liquid crystal molecules can be changed by applying voltage, thereby regulating the transparency of the device.[205] (d) When voltage is applied, the device changes from opaque to transparent.[205] (e) Schematic illustration of an electro-zoom device. When a voltage is applied, the two gel layers squeeze the dielectric elastomer by electrostatic force to flatten the lens and increase the focal length.[207] (f) With the help of an electro-zoom device, the quality of the image can be regulated by adjusting the voltage.[207]

active layer, causing the device to emit light or change transparency (Fig. 13d). The similar structure of the capacitive optoelectronic effector and the capacitive sensor suggests its possibility as a dual-function device for sensing and feedback.

The electro-zoom device with adjustable focal length is realized by a capacitive actuator.[207] Like the human eye, the dielectric elastic body acts like a muscle, and the ion gel acts as the lens and the nervous system for zooming and signal transmission (Fig. 13e). Benefitting from the advantages of stretchable and transparent ionic hydrogels, the optical zoom effector exhibits a powerful adjustable optical performance (Fig. 13f). The ion eye shows fast responses (3.6 ms) and a wide range of focal length changes (approximately 50%). By combining with more ionic sensors, an electro-zoom device is expected to be used in bionic robots and medical treatments based on ion sensor systems as an ionic eye.

7. Hydrogel ionic power sources

Hydrogel ionic sensor systems are inherently flexible, which has increased the demand for essential energy supply equipment that maintain high performance and safety under various deformations, and therefore puts forward higher requirements for the internal component performance and interface combination of energy storage devices. Hydrogel ion power sources came into being based on this demand. Our discussion of hydrogel-based power sources is organized into two sections, energy storage devices and energy harvesters (Table 3).

Table 3 Comparison of the performance of different hydrogel ionic power sources

Battery type	Operating voltage (V)	Specific capacity (mAh g^{-1})	Cycling performance	Ref.
Stretchable Li-ion battery	1.7	28	50 cycles with 65% capacity	Chen *et al.*[208]
Aqueous Na-ion battery	1.03	160	100 cycles with 90% capacity	Zhang *et al.*[209]
Quasi-solid-state Li-ion battery	3.4	160	300 cycles with 98.9% capacity	Jiang *et al.*[210]
Wearable Zn-ion battery	1.5	306	1000 cycles with 97% capacity	Li *et al.*[211]
Ultralong-life Zn-based battery	1.6–1.8	260	16 000 cycles with 65% capacity	Huang *et al.*[212]

7.1. Energy storage devices

Currently, the most common flexible energy storage devices are batteries and supercapacitors. Electrolyte is an important element that determines the level of the electrochemical window and ion transmission efficiency of a battery or supercapacitor. Conventional flexible batteries or supercapacitors rely on membranes permeated with liquid electrolytes to act as solid electrolytes. However, there are clear drawbacks to this type of electrolyte: low ionic conductivity, poor mechanical strength, and high risk of short circuit.[213] At the same time, most electrolyte solvents are toxic and flammable organic solvents. Compared with organic solvent electrolytes, aqueous electrolytes have outstanding advantages in terms of safety and environmental performance. The ion-conducting hydrogel containing large amounts of aqueous electrolyte offers an ideal electrolyte with flexibility, high ionic conductivity, and high safety for flexible energy storage devices. As shown in Fig. 14a, a hydrogel acts as both an electrolyte and a diaphragm to prevent short circuit caused by the contact between the cathode and the anode.

A battery is a device that stores energy in the form of chemical energy. They have sufficiently high energy density and are suitable for long-term energy storage. At present, common batteries based on hydrogel electrolytes include lithium ion batteries, sodium ion batteries and zinc ion batteries.

Lithium-ion batteries (LIB) are widely used due to their high energy density (200 W h kg^{-1}), high power density (10 kW kg^{-1}) and long-term stability (delivered 200 mA h g^{-1} for 100 cycles).[214] Sodium-ion batteries (SIB) have attracted extensive attention as an alternative method of lithium ion energy storage technology due to their rich composition and low cost.[215] With the rapid development of flexible and wearable electronic devices, in addition to achieving higher energy density and longer service life, the development of flexible lithium or sodium ion energy storage technology has become an emerging research field.[216] However, the high cost and safety issues brought about by the organic solutions used in lithium-ion and sodium-ion batteries prompt the development of alternative energy storage solutions.[217] The use of safe and relatively inexpensive hydrogel electrolytes instead of flammable and expensive organic electrolytes is a competitive candidate.[210,213,218,219] The main bottleneck of the application of hydrogels to lithium-ion batteries and sodium-ion batteries is that the electrochemical window of the aqueous electrolyte is very narrow (1.23 V), which limits the performance of batteries. To solve this dilemma, revolutionary "water-in-salt" electrolyte (WiSE) is introduced into hydrogels to prepare high-performance lithium-ion batteries. As an example, a polyacrylamide hydrogel containing WiSE can provide a working window of 3.28 V (1.95 to 4.93 V).[208] On the other hand, the electrochemical window is significantly expanded as the polymer content increases, because the polymer network appropriately restricts the movement of water molecules, thereby inhibiting water-induced side reactions, including hydrogen release and passivation.[56] The electrochemical window of the hydrogel electrolyte with a polymer content exceeding 55% can be extended to 5 V.[209]

Zinc-ion batteries (ZIB) are inherently safe and environmentally friendly, because they are not subject to environmental restrictions of anhydrous and/or anaerobic assembly and are suitable for aqueous electrolyte environments. The high natural abundance of zinc is conducive to large-scale and low-cost production. Due to their low electrochemical potential (−SHE of −0.76 V) and high capacity (5850 mAh cm^{-3}), zinc-ion batteries are considered to be the most promising alternatives to commercial lithium-ion batteries and show the greatest promise for future energy applications.[220,221] For instance, a polyacrylonitrile electrospun fiber membrane filled with gelatin modified by polyacrylamide plays the role of hierarchical structured hydrogel electrolyte, which was further assembled into a flexible Zn–MnO_2 rechargeable battery with outstanding safety.[211] Flexible solid-state ZIBs can provide a high power density of 148.2 mW cm^{-2}. The thickness of the entire device is close to that of a piece of A4 paper. More importantly, a solid ZIB exhibits extremely high safety performance when it is used in various harsh environments, such as being bent, hammered, punctured, cut, sewed, washed in water and put on fire (Fig. 14b). As another example, a sodium polyacrylate hydrogel electrolyte was applied to solid Zn//NiCo and Zn–air batteries which exhibited ultralong lifetimes and high capacities.[212] Thanks to the inherent high ionic conductivity of 0.17 S cm^{-1} and strong water-retaining capacity of the sodium polyacrylate hydrogel electrolyte, the prepared battery exhibits a high electrical capacity (Zn//NiCo battery – ≈ 260 mAh g^{-1}, Zn–air battery – ≈ 800 mAh g^{-1}), ultra-long cycle stability (the Zn//NiCo battery has a capacity of 16 000 cycles of 65% and the Zn–air battery withstands 800 cycles of 160 h).

Supercapacitors have high power densities and the ability to charge and discharge rapidly. There are two ways to store energy in supercapacitors. The first is through the surface adsorption of electrolyte ions (as in electric double layer capacitors).[222,223] The electrodes of this type of capacitor are generally carbon materials. Its performance is related to the

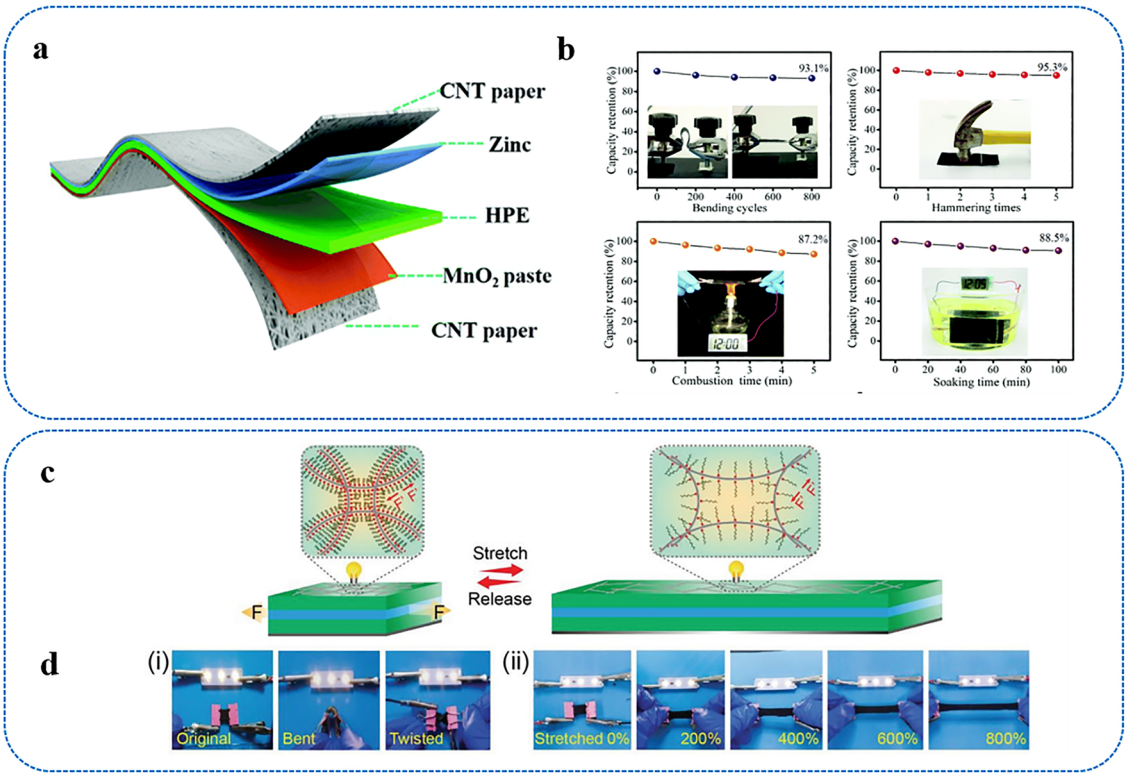

Fig. 14 Hydrogel energy storage devices. (a) Schematic illustration of the structure of the solid-state ZIB. The hydrogel acts as both an electrolyte and a diaphragm to prevent short circuit caused by the contact between the cathode and the anode.[213] (b) The hydrogel-based flexible ZIB can work normally under various severe tests.[213] (c) Schematic diagram of a stretchable supercapacitor based on a hydrogel. The hydrogel electrolyte and electrodes maintain superior stability during the process of stretch–release.[230] (d) A supercapacitor powers LEDs under various deformation and stretching procedures.[230]

effective surface area of the electrode. The second type of supercapacitors store electrical energy through fast surface redox reactions (pseudocapacitors),[213,224] whose electrodes mainly include transition metal oxides and conducting polymers, and their performance is closely associated with the electrode materials. As shown in Fig. 14c and d, by combining flexible electrodes (such as carbon cloth loaded with active electrode materials), solid-state supercapacitors based on ionic hydrogel electrolytes can maintain stable electrical performances under deformation.[64,225]

Adding additional functions to energy storage devices, through the design of devices and hydrogel materials, can make them highly versatile for use in complex working environments. For example, by combining intrinsic or structural stretchable electrodes, stretchable batteries or capacitors can be prepared.[226–229] Purposeful design and preparation of hydrogels can endow energy storage devices with functions of self-healing,[230–232] antifreeze,[233–235] shape memory,[236,237] protection from overheating,[238–240] and self-discharge suppression.[241]

7.2. Energy harvesters

Hydrogel ionic sensor systems need portable and sustainable power sources. Energy storage devices have a limited lifetime and present potential hazards to health and the environment. The significant development of sensing equipment urgently requires the development of new technologies that can obtain sustainable energy from the environment. Hydrogel-based energy harvesters are used to collect energy wasted in the environment and convert it into electrical energy. Currently, the harvesters mainly collect three forms of energy: chemical energy, mechanical energy and salinity gradient energy.

Atmospheric moisture is a ubiquitous and sustainable energy source that has recently attracted increasing interest for decentralized energy harvesting.[242] Ionic hydrogel-based moisture-electric generators (MEGs) convert chemical energy directly into electricity *via* functional material–humidity interactions, offering a different energy conversion pathway from conventional photovoltaic or thermoelectric systems. For example, by introducing ionic liquids into the double-network hydrogel system formed by poly(2-acrylamido-2-methylpropanesulfonic acid) (PAMPS) and polyvinyl alcohol (PVA) to induce microphase separation, PAB ionogels can be obtained, thereby constituting the PAB-MEG system (Fig. 15a).[243] The PAB-MEG system can achieve stable power transmission without the need for external energy storage or rectifier circuits. In practical tests, a 1 × 4 series-integrated PAB-MEG array can charge a smartwatch based on motion, providing a 100 hour battery life (Fig. 15b).

Triboelectric nanogenerators (TENGs) are mainly based on contact electrification and electrostatic induction to realize the

conversion of mechanical energy into electrical energy. During the periodical contact and separation of the object with the TENG, ions flow repeatedly in the hydrogel and induce the external load to generate an alternating current through capacitive coupling (Fig. 15c). The ion-conducting hydrogel TENG can output electricity with an instantaneous peak power density of 35 mW m^{-2}, which is close to that of TENGs based on electronic conductors, and converts energy through human motion to drive wearable electronics (Fig. 15d).[244,245] Ionic hydrogel-based TENGs have the advantages of large output power, light weight and simple manufacturing, while also exhibiting high stretchability and transparency.[245–249]

Dielectric elastomer generators (DEGs) are also used for the collection of mechanical energy, and are composed of a dielectric elastomer film sandwiched between two ion-conducting hydrogels (Fig. 15e).[250,251] The dielectric elastomer generator will absorb the charge from the external power source to increase the capacitance during the stretching state. When the power is disconnected and the DEG is released, the capacitance of the DEG decreases with the elastic recovery of the shape, resulting in an increase in the voltage between the electrodes. Many studies have shown that the efficiency of energy conversion of DEGs can be effectively improved by equi-biaxial stretching (Fig. 15f). The capacitance C scales with the fourth power of stretch ratio λ: $C \propto \lambda^4$.[252–254]

The salinity gradient between river water and sea water is a potential renewable energy source.[255,256] The desire to collect clean energy from water to replace fossil fuels has promoted the development of salinity gradient energy harvesters. The electric eel inspired a new type of hydrogel-based energy harvester that uses ion gradients to collect energy.[257] The power source is created by sequentially stacking a high salinity hydrogel, a cation selective hydrogel, a low salinity hydrogel, an anion selective hydrogel, and a second-high salinity hydrogel (Fig. 15g). The selective diffusion of ions creates an ion gradient to generate energy, which can generate a voltage of up to 110 V by stacking the units in series (Fig. 15h). By increasing the asymmetry between the membrane layers, the unidirectional ion diffusion can be effectively promoted, resulting in an increase in the ability to use the difference in ion concentration to generate electricity. A heterogeneous membrane made of polyanion electrolyte hydrogel and porous aramid nanofiber (ANF) is used to generate electricity *via* salinity gradients (Fig. 15i).[258] Inherent synergistic effects of static electricity, chemistry, and structural asymmetry make the system have a stable ion diode effect, which greatly promotes the unidirectional transmission efficiency of cations to enhance the power generation (Fig. 15j). The power output of heterogeneous membranes has been significantly increased to $\sim$5.06 W m^{-2}.

Despite the rapid development of hydrogel-based energy harvesters, power output and energy conversion efficiency remain key limiting factors for practical applications. In most cases, the generated power density is still relatively low and highly dependent on external stimuli such as mechanical motion, thermal gradients, or environmental humidity, resulting in intermittent and unstable energy supply. This limitation originates from the fundamental working mechanism of ionic power generation, which relies on ion diffusion, charge separation, and concentration gradients rather than fast electron transport.[259] Therefore, the energy conversion process is inherently diffusion-limited and exhibits relatively slow response dynamics, which is consistent with ionic energy harvesting systems, where device performance and power output are fundamentally governed by ion transport kinetics.[260] Such characteristics restrict the ability of these systems to continuously power integrated electronic components. These constraints have been widely recognized in ionic energy systems, where power generation is often governed by ion transport kinetics and environmental conditions.[166]

8. Aging mechanisms and stability enhancement strategies of hydrogel ionic systems

Hydrogel-based ionic systems exhibit excellent mechanical compliance, ionic conductivity, and biocompatibility. However, their long-term stability remains a critical challenge that limits practical deployment, particularly under real-world environmental and operational conditions. The aging of hydrogel ionic systems generally originates from three primary mechanisms: dehydration, ion leaching, and mechanical fatigue. Understanding these degradation pathways is essential for the rational design of durable ionic devices.

8.1. Dehydration-induced performance degradation

Dehydration is one of the most fundamental aging mechanisms in hydrogels due to their intrinsically high water content. When exposed to ambient or elevated temperatures, water evaporation leads to significant shrinkage of the polymer network, resulting in increased stiffness, reduced elasticity, and diminished ionic conductivity.[261]

More importantly, dehydration alters the microstructure of hydrogels by collapsing ion transport pathways and increasing ion–polymer interactions, thereby severely suppressing ion mobility.[262] In extreme cases, dehydration-induced stress can even lead to crack formation or structural failure. Additionally, under freezing conditions, localized dehydration driven by ice formation (cryosuction) can further induce fracture and irreversible damage, highlighting the coupled effects of dehydration and environmental stress.[263]

To address dehydration, several approaches have been developed. For instance, coating hydrogels with elastomeric or polymeric barrier layers effectively reduces water evaporation and enhances environmental stability.[262] As another example, replacing part of water with hygroscopic solvents can significantly suppress evaporation and maintain conductivity.[264]

8.2. Ion leaching and compositional instability

Another critical aging pathway is ion leaching, particularly in open or bio-interfaced systems. Due to concentration gradients between the hydrogel and surrounding media, mobile ions

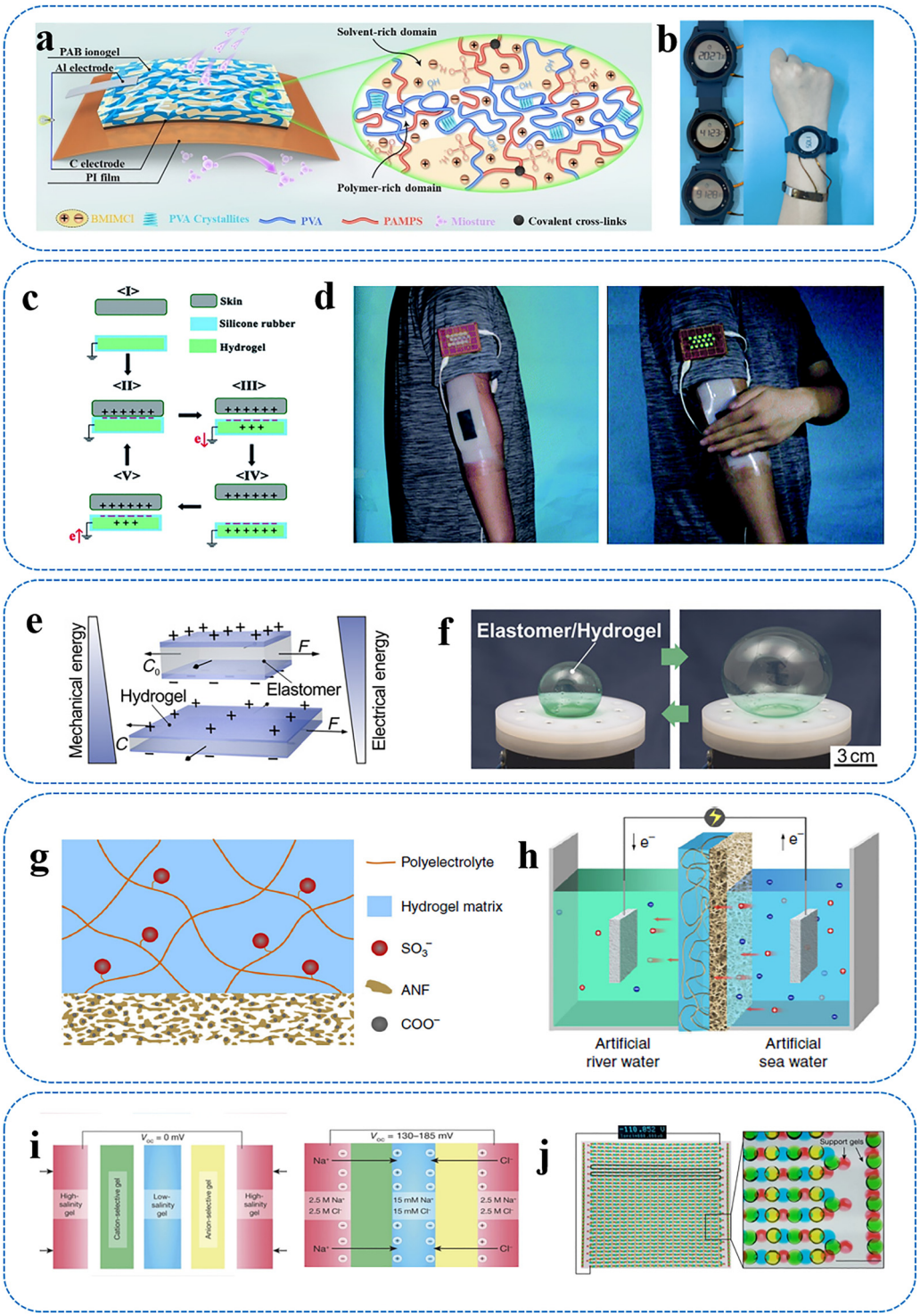

Fig. 15 Hydrogel energy harvesters. (a) Schematic diagram of one-single PAB-MEG device with asymmetric moisture penetration layers.[243] (b) Integrated PAB-MEGs harvest moisture energy to power a watch.[243] (c) Schematic diagram showing the working principle of a hydrogel-based TENG in the single-electrode mode. The TENG converts mechanical energy into electrical energy through contact charging and electrostatic induction.[245] (d) A TENG harvested the energy of percussion to power the LEDs.[245] (e) Schematic illustration of the working mechanism of a dielectric elastomer generator. A dielectric elastomer generator can convert mechanical energy into electrical energy through the capacitance change caused by stretching.[250] (f) An efficient energy conversion rate of 11% can be effectively achieved by inflating the balloon.[250] (g) Schematic illustration of a hybrid membrane with an asymmetric structure composed of a polyelectrolyte hydrogel and aramid nanofiber membrane.[258] (h) Schematic of the osmotic energy conversion process.[258] (i) Schematic illustration of the working mechanism of an all-gel energy harvester of salinity gradient. The selective diffusion induced by hydrogels with different concentrations and ion types would convert the salinity gradient into electrical potential differences.[257] (j) The voltage of the energy harvester in series can be up to 110 V.[257]

tend to diffuse outward, leading to gradual depletion of charge carriers.[31] This process results in reduced ionic conductivity, signal drift, and degraded device performance over time. Ion leaching is especially problematic in bioelectronic interfaces and aqueous environments, where continuous ion exchange can disrupt both device functionality and biological compatibility. Moreover, leaching may alter the internal ionic balance, affecting electrochemical stability and device reproducibility.[265]

To mitigate ion leaching, substantial efforts have been devoted to regulating ion transport and confinement within hydrogel networks. One effective strategy involves the incorporation of fixed charges through polyelectrolyte or zwitterionic architectures, which can immobilize counterions and suppress their outward diffusion by electrostatic interactions.[266] In addition, spatial confinement approaches such as aqueous two-phase systems (ATPS) enable the localization of conductive ionic species within distinct domains, thereby maintaining high ionic conductivity while minimizing ion exchange with the surrounding environment.[158] Furthermore, physical encapsulation using elastomeric or polymeric barrier layers has been widely adopted to isolate hydrogels from external media, effectively reducing electrolyte leakage and preventing instability or even short-circuit risks in aqueous systems.[267] Collectively, these strategies highlight the importance of controlling ion mobility and interfacial exchange to ensure long-term compositional stability of hydrogel ionic systems.

8.3. Integrated strategies for long-term stability

In practical applications, these aging mechanisms often occur simultaneously and are strongly coupled. For example, dehydration can significantly alter the microstructure of hydrogel networks by reducing water content and increasing polymer chain density, which in turn affects mechanical properties and may accelerate fatigue-induced damage.[268] Meanwhile, dehydration driven by osmotic imbalance or environmental exposure can lead to structural shrinkage and failure, further exacerbating mechanical instability.[262] In parallel, ion transport and retention in hydrogels are intrinsically governed by diffusion and thermodynamic equilibrium, implying that ion leaching can disrupt the internal ionic balance and indirectly influence mechanical integrity and electrochemical stability.[269] These coupled effects highlight that individual degradation pathways cannot be considered in isolation.

Therefore, future designs should adopt multifunctional and synergistic strategies, integrating multiple stabilization mechanisms within a single system. For instance, combining encapsulation layers to suppress water evaporation and ion exchange, anti-freezing or anti-dehydration solvent systems to maintain hydration under extreme conditions, and dynamic or self-healing polymer networks to resist mechanical fatigue, represents a promising direction for achieving durable performance. Such integrated designs enable simultaneous regulation of water retention, ion transport, and network integrity, thereby addressing the interdependent nature of hydrogel aging processes.

9. Future development directions for hydrogels

Based on the unique properties of hydrogels, various innovative hydrogel ionic sensing devices have been constructed. However, in the face of broad development prospects, the properties of hydrogels should be continuously improved to meet more comprehensive needs and develop new functions to open untapped opportunities. We will discuss future research directions for hydrogels on three major aspects (Fig. 16): (1) development of hydrogels with extraordinary properties, (2) integration of hydrogels and (3) weather resistance improvement of hydrogels.

9.1. Hydrogels with extraordinary properties

9.1.1. Hydrogels with high strength and high toughness. Demonstrating strength and toughness in hydrogels at the same time, which are usually contradictory mechanical properties, is beneficial to prolong service periods, endure high loads and large deformation, and improve impact resistance.

By introducing the energy dissipation mechanism during the loading process into hydrogels, for example including dual-network hydrogels,[45,270,271] hydrogels with chemical and physical hybrid crosslinking agents,[272,273] creating nanocrystalline domains[274,275] or improving the homogeneity of the hydrogels, with examples including topological hydrogels with sliding crosslinkers,[276,277] and tetra-arm polymer hydrogels,[278] many hydrogels have shown tremendous enhancements in strength and toughness compared with their conventional counterparts.

A breakthrough strategy to produce ultra-strong nanocomposite gels with highly ordered layered structures has been proposed (Fig. 16a).[279] At the immiscible hydrogel/oil interface, two-dimensional nanosheets are arranged in an orderly manner under the induction of shearing force in the hydrogel prepolymerization solution and polymerized. An appropriate weight percentage of the nanosheets would cause the polymer chains to harden effectively under the strong constraints of the nanosheets. The gel reinforced by two-dimensional nanosheets exhibits high strength of up to 1215 ± 80 MPa and a toughness of up to 36.7 ± 3.0 MJ m^{-3}. This work provides a generic and facile approach for generating high-strength and high-toughness composite materials.

High strength nanocomposite polymers can also be fabricated *via* an interfacial co-crystallization strategy. For instance, Liu *et al.* constructed a sub-molecularly flat interface between ferromagnetic vanadium diselenide (VSe_2) and ferroelectric poly(vinylidene fluoride) (PVDF) nanocrystals, resulting in a high-performance magnetoelectric polymer composite (Fig. 16b).[280] The obtained material exhibits a tensile strength exceeding 100 MPa and a magnetocapacitive coefficient of 23.6%, demonstrating outstanding mechanical robustness and magnetoelectric coupling. Owing to these advantages, this

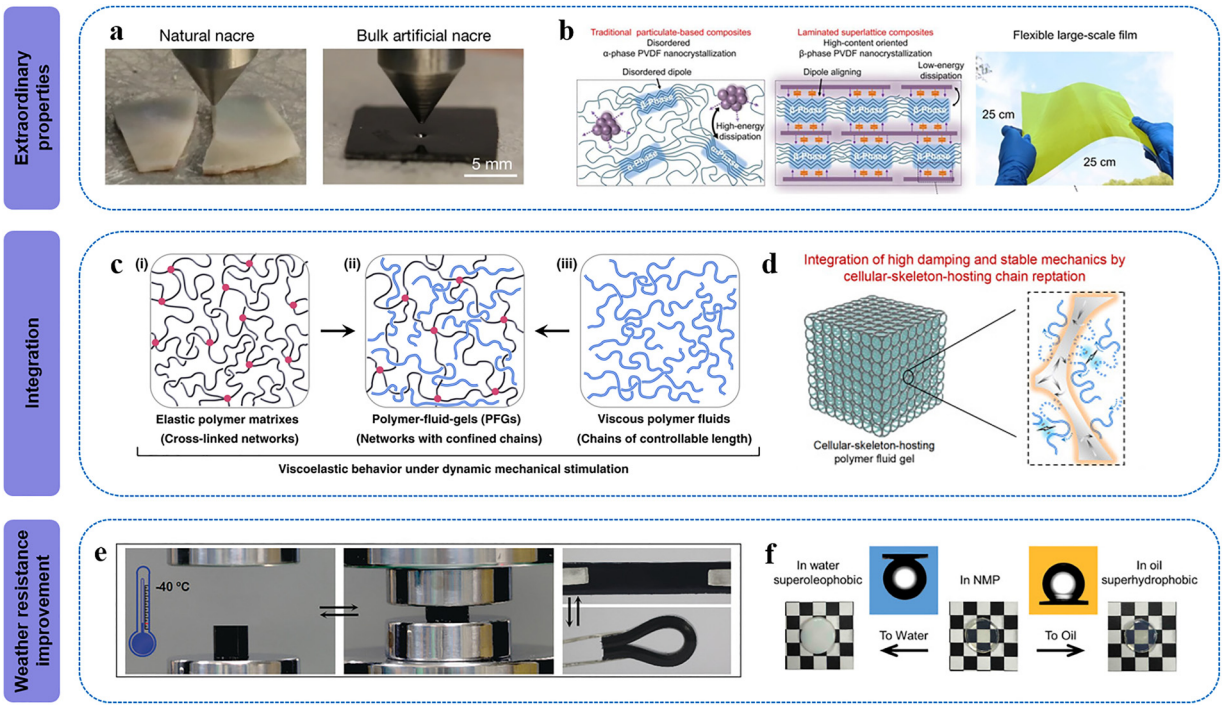

Fig. 16 Future development directions for hydrogels. (a and b) Hydrogels with extraordinary properties: (a) high strength and toughness nanocomposite gel.[279] (b) High strength and magnetoelectric performance nanocomposite polymer.[280] (c) and (d) Integration of hydrogels: (c) construction of polymer–fluid–gels.[332] (d) Cellular-skeleton-hosting polymer fluid gel.[331] (e) and (f) Weather resistance improvement of hydrogels: (e) enhanced temperature adaptability of hydrogels;[119] (f) enhanced swelling resistance of hydrogels.[337]

composite shows great potential for applications in wearable magnetoelectric sensors.

9.1.2. Programmable hydrogels. At present, hydrogel materials lack the ability to control and adjust their mechanical properties stably, which limits their engineering applications in complex environments.[281] In nature, many biological soft tissues with synergistic heterostructures, such as sea cucumbers, skeletal muscle and cartilage, can adapt to complex environments by adaptive mechanical properties.[282–284] Inspired by them, the researchers designed and prepared a heterogeneous gel network with excellent mechanical adaptability.[285–288] Incorporating oil-phase monomers with phase change behavior triggered by temperature into hydrogels, renders hydrogels with excellent switchable mechanical and shape memory properties.[285] By using this strategy on a metal-supramolecular hydrogel framework, a dual-programmable shape-deformable organic hydrogel was further prepared.[286] In order to break through the simple bistable mechanical state of rigid and soft, a variety of non-eutectic phase transition components are incorporated into continuous elastic hydrogel networks to construct a programmable organic hydrogel with multi-stable mechanical states. A multi-programmable hydrogel can stably switch mechanical modulus in a stepwise manner under heat induction (*i.e.*, triple, quadruple, and quintuple switching).[287] Smart hydrogels with precisely controllable mechanical properties provide valuable breakthroughs in practical applications, including wearable devices, biomedical engineering, and soft robots.[289–291]

9.1.3. Self-healing hydrogels. Biological organisms have built-in repair mechanisms to ensure stable physiological functions.[292] For example, human skin produces collagen through the stimulation of inflammation to regenerate epithelial cells and tissues.[293] Plants can induce repair through oligopeptides, oligosaccharides or other molecules.[294] Development of self-healing materials can not only extend the service life of the material, but also improve the reliability of the material by avoiding failures caused by the accumulation of cracks.[295] Abundant functional groups endow the hydrogel materials with great designability and allow them to have fast self-healing properties after being purposefully designed. There are two main repair mechanisms of self-healing hydrogels: dynamic covalent reactions (chemical cross-linking) and non-covalent reactions (physical cross-linking).[296] Common cross-hydrogels are cross-linked by irreversible chemical bonds, so it is difficult for hydrogels to self-healing. The dynamic covalent bonds are not permanently cross-linked, as they can reversibly recombine after breaking. Reactions that can form dynamic covalent bonds include phenylboronic acid complexation reactions,[297,298] disulfide bonds,[299,300] imine bonds,[301,302] acylhydrazone bonds,[303,304] and Diels–Alder reactions[305,306] and others. The process of repairing hydrogels based on dynamic covalent bonds often requires the application of external stimuli, such as UV light,[230] alternating current[307] and pH.[308] In the case of physically self-healing hydrogels, noncovalent interactions are generally utilized, such as hydrogen bonds,[308,309] hydrophobic interactions,[310] host–guest interactions,[311] ionic

interactions,[312] nanocomposite effects,[313] crystallization effects[314,315] and π–π stacking effects.[316] The durability and stability of various flexible devices based on self-healing hydrogels are greatly improved, which also means less energy consumption and less waste generation.

Without introducing new functional groups and special designs, the method of preparing self-healing hydrogels by increasing the preparation temperature provides valuable insight.[317] A hydrogel prepared at high temperature contains a loose network of highly mobile short polymer chains, which can promote the exchange of hydrogen bonds to facilitate self-healing. It exhibits rapid self-healing properties at room temperature (below its T_g).

9.2. Integration of hydrogels

9.2.1. Functional integration of hydrogels. In order to meet more complex and comprehensive application requirements, the multi-functionalization of hydrogel-based equipment is the future development trend. A large number of integrated applications have been explored.[318] For instance, various stimulus-sensitive sensors are integrated to mimic the mechanical, temperature, and humidity receptors of human skin, respectively.[319] Integrating flexible powers into the self-charging devices in the system can remove the limitation of the fixed power.[227,320] The introduction of wireless communication devices such as WiFi transmitters into the flexible strain sensor enables human movement to be effectively detected remotely, which improves portability and comfort.[321] Hydrogels with multiple functions are coupled into an integrated system of soft robots that can perform complex actions.[322,323] For example, magnetic particles are introduced into a temperature-sensitive hydrogel head as a magnetic drive unit, and a non-magnetic hydrogel tail as a functional unit to obtain a segmented hydrogel robot that can carry out multimodal motion.[322] These sophisticated hydrogel soft robots are envisioned to be used in medical operations.

9.2.2. Materials integration of hydrogels. A complete hydrogel-based device usually consists of multiple materials with corresponding functional merits. Therefore, the adhesion of hydrogels to different materials (*e.g.*, elastomers, metals, and glass) is a key factor that determines the stability of devices.[31] Among them, the adhesion between hydrogels and elastomers is the most notable.[1] Elastomers with low water and solute permeability are equivalent to coats for hydrogels, which can effectively prevent the dehydration of hydrogels or the exchange of substances with the external environment when the device is immersed in solution, thereby improving the mechanical reliability of hydrogels under harsh temperature and chemical conditions. Conversely, hydrogels as a coating for elastomers such as medical catheters can provide a biocompatible interface while reducing mechanical mismatch and foreign body reactions.[324,325] Currently, the interfacial adhesion of hydrogels is mainly achieved through physical interaction,[326,327] covalent anchoring,[328,329] and interfacial interpenetration.[50,324,330]

Compared with physical interactions based on weak non-covalent bonds such as electrostatic interactions and hydrogen bonds, the interface formed by covalent anchorage is more stable. As an example, an unreacted double bond can be introduced into a hydrogel by reacting the hydroxyl group with acryloyl chloride.[328] The organogel–hydrogel hybrid is obtained by polymerizing organogel monomers onto the surface of the modified hydrogel. However, the low toughness and brittle interfaces formed by covalent anchoring will still crack under high mechanical load.

The method of interfacial interpenetration makes the two polymer networks produce molecular entanglement to obtain a firm interface, which is strong enough to elicit the Lake-Thomas mechanism and significant hysteresis in the bulk. The interpenetration of stitching polymers (such as silane coupling agents) can bridge hydrogels and elastomers to improve adhesion.[330] The silane coupling agent is added to the precursor of both the hydrogel and elastomer. During the manufacturing process of the polymer, the reactive silane coupling agent produces a strong bond on the interface. Alternatively, adhesion can be improved by using benzophenone to modify the permeability of the elastomer surface to hydrophilic polymers and monomers, which allow the hydrogel network to interpenetrate into the elastomer surface to form a firm bond.[325]

In addition, the integration of elastic networks with gels can also be achieved by infiltrating high energy-dissipative polymeric fluids into an elastic polymer matrix (Fig. 16c and d).[331,332] For example, Liu *et al.* prepared polymer-fluid-gels (PFGs) by photoinitiated free-radical polymerization of a prepolymer solution containing *n*-butyl acrylate monomer, poly(*n*-butyl acrylate) (PBA) fluid, ethylene glycol dimethacrylate, and 2,2-diethoxyacetophenone.[332] The resulting PFGs exhibit pronounced energy dissipation over a broad frequency range (10^{-2}–10^{8} Hz), with loss factors exceeding 0.5, demonstrating their potential as high-performance impact-resistant materials. Owing to this combination of high dissipative capacity and elastic integrity, PFGs show promise for applications in actuators, wearable devices, flexible electronics, and soft robotics.

9.3. Weather resistance improvement of hydrogels

9.3.1. Improvement in anti-swelling properties. Considering that hydrogels will be used *in vivo*, in high humidity environments and even underwater in the future, its anti-swelling performance should be significantly improved. The difference in osmotic pressure causes the swelling of hydrogels.[333,334] Swelling significantly weakens the mechanical toughness and limits the applicability of hydrogels.[90,333] The development of anti-swelling hydrogels becomes an important but challenging proposition. The degree of swelling is mainly affected by the hydrophilicity of the polymer and the cross-linking degree.[90] Bearing in mind the impact of hydrophilic polymers, a heteronetwork organohydrogel is obtained by combining the oleophobic polymer network and hydrophobic polymer network to limit the swelling.[335,336] Because of the mutual restriction between the two networks, the organohydrogel can maintain its original volume in various immersion environments with different hydrophilic and hydrophobic

properties. At the same time, the integration of a heteronetwork endows organohydrogels with adjustable hydrophobic and oleophobic properties according to the soaking environment and stable elasticity over a wide temperature range. For example, the poly(vinyl alcohol)/poly(butyl methacrylate)-*co*-poly(lauryl methacrylate) multiple network organohydrogels (MN-OHGs) prepared by Liu *et al.*[337] When the ratio of the oleophilic polymer network (OPN) to the hydrophilic polymer network (HPN) is 2/1, MN-OHGs can maintain the same swelling ratio in water and *n*-dodecane. Moreover, the surface of MN-OHGs can dynamically transition between hydrophobic (in oil) and oleophobic (in water) states (Fig. 16e). The way to control swelling by introducing thermoresponsive segments is also worth learning. When the temperature increases to the critical temperature (T_c), the hydrophobic effect caused by the thermoresponsive segments will dominate, causing a sharp shrinkage of the hydrogel volume.[333] On the other hand, enhancing the degree of crosslinking of hydrogels is also an effective method for inhibiting swelling of hydrogels. For example, coordination bonds or hydrogen bonds have been introduced into the network of a crosslinked hydrogels to form a dual-crosslinked hydrogel, which has a significantly reduced swelling rate while exhibiting excellent mechanical strength in a balanced swelling state.[338–340] In addition, a collaborative strategy of combining organohydrogels and dual-crosslinked hydrogels can also effectively achieve the effect of inhibiting swelling.[334]

9.3.2. Improvement in temperature adaptability. Conventional hydrogels contain a large amount of water, which inevitably freezes resulting in a loss of flexibility and limiting the transport of ions in sub-zero temperature environments and dehydration at high temperatures, which seriously affect the performance of hydrogel-based devices. The freezing of water at low temperatures is a crystallization phenomenon caused by strong hydrogen bonds between water molecules.[341]

Methods to inhibit the freezing of hydrogels can be divided into two categories: The first type of mechanism is to introduce additives to combine with water molecules to weaken the interaction between water molecules. This method can reduce the freezing point of the aqueous solution. Specific solutions include adding ionic salts[342–345] or organic solvents.[119,233,234,346] An antifreeze hydrogel maintains flexibility at −57 °C through the addition of $CaCl_2$ (when $CaCl_2$ is 30 wt %).[342] Liu *et al.* added ethylene glycol to the PVA hydrogel to prepare a conductive hydrogel that has stable flexibility and a high ion conductivity of 2.38 mS cm^{-1} at −40 °C (Fig. 16f).[119]

The second option is to introduce nano-constraints of water molecules to inhibit the ice recrystallization and growth. Studies have shown that hard confinement of water clusters smaller than 10 nm can effectively prevent water crystallization.[347,348] Therefore, the introduction of a hard polymer network structure into the hydrogel is also conducive to enhancing its antifreezing properties.

By introducing a lipophilic network that reduces the size of ice crystals into the hydrogel network to suppress water crystallization, the antifreeze hydrogel maintains a stable modulus over a wide range of temperatures, from −78 °C to 80 °C.[335]

Hydrogels are susceptible to dehydration in air, and the increase in temperature will accelerate the dehydration process, which is also a bottleneck in its application. Owing to the strong interaction of the above-mentioned ionic salt and organic solvent resulting in anti-freeze abilities, they can effectively stabilize water and prevent the volatilization of water.[343,346] Encapsulating a hydrogel with an elastomer film can also effectively weaken the exchange of substances between the hydrogel and the outside world, thereby reducing water loss.[324,349]

10. Conclusions and outlook

We have focused on the unique performance and working mechanisms of hydrogel-based sensing systems, as well as their potential applications. Although various functions of ion transport have been achieved based on hydrogels, the field is still in its infancy and has ample room for future development. Here, we will discuss the challenges faced by the hydrogel ion transport systems from four aspects: improving selectivity, synergy and systematization, bionic intelligence, and enhancing performance.

10.1. Improving selectivity

The protein channel can precisely control the opening and closing of the channel under the synergistic effect, performing the selective input and output of Na^+/K^+ ions into the cell to further perform the generation and conduction of nerve impulses.

However, the ion selectivity and rectification of the hydrogel ion sensor system can only be limited to the choice of anions and cations. The separation of lithium in magnesium/lithium brine using nano-heterogeneous membranes has given us enlightenment, but there are still limitations.[350] Solving the above insurmountable challenges will help to realize more advanced ion sensing functions.

Numerous receptors in the human body can clearly distinguish a variety of stimuli. In order to realize this multi-stimulus perception, integrated sensors have been developed. However, the current sensor systems lack a differentiated monitoring mechanism for different stimuli, which leads to the generation of stimulus interference. How to accurately distinguish multiple stimuli simultaneously to meet reliable sensing requirements is a challenging topic.

10.2. Inter-module coupling challenges

Hydrogel-based ion sensing modules (sensors, transporters, processors, effectors, and power sources) have shown unique effects in many aspects. However, we cannot ignore that its systematic research progress remains in its infancy. The practical implementation of hydrogel ionic sensory systems critically depends on the efficient coupling between these modules.

Nevertheless, fundamental differences in charge carriers, transport mechanisms, and interface properties introduce several key challenges, including impedance mismatch, signal attenuation, and cross-interference.

To address these challenges, several strategies have been explored. Structurally, designing graded or hybrid interfaces can reduce impedance mismatch and enhance charge transfer efficiency.[1,351] Functionally, ion-selective channels, nanoconfined pathways, and heterostructured hydrogels can regulate ion transport and suppress signal dispersion.[352] Additionally, encapsulation strategies and multi-phase systems can minimize ion leakage and environmental interference, thereby improving signal stability.[353] Finally, integrating signal amplification and rectification units within the system can compensate for signal attenuation and enhance overall robustness.[354]

Overall, achieving seamless coupling between modules remains a central challenge for hydrogel ionic sensory systems. Future progress will rely on the co-design of materials, interfaces, and device architectures to enable efficient, stable, and low-noise signal transmission across multi-component ionic circuits.

10.3. Bionic intelligence

Imitating creatures to make autonomous decisions is the future development direction of intelligent systems. On the one hand, studies have confirmed that animals can respond to stimuli through an autonomous, non-centrally controlled system. Thus, the dynamic structure of the ionic decision maker is expected to achieve adaptive decision-making of the system, which will significantly reduce computing requirements and simplify systems. On the other hand, the combination of machine learning can help the hydrogel ion sensing systems make decisions with minimal human interference by learning from data. A more autonomous and self-improving sensor system will perform tasks in a smarter way.

10.4. Enhancing performance

There is ample room for improvement in the performance of hydrogels in numerous applications. For example, the ion conductivity (10^{-3}–10^{3} S m^{-1}) and thermal conductivity of hydrogels ($\sim$0.6 W m^{-1} K^{-1}) are much lower than those of metals; the electrochemical window of hydrogels is narrow, which makes it difficult to meet high-voltage direct current applications; compared to inorganic nanomaterials, the sensitivity of hydrogel-based strain sensors is comparatively low; the power density of the hydrogel actuator is only in the range of 0.1 to 10^{3} W m^{-3}, which is far from the actuation power density of mammalian skeletal muscle. Breaking through the aforementioned challenges in the performance of hydrogels will effectively extend the range of applications of hydrogels sensing systems.

With the development of hydrogel-based ion sensing technology, more ''human-like'' devices will appear. By integrating these devices, a mature hydrogel ion sensory system will be established, which can operate seamlessly between artificial machines and biological systems.

Conflicts of interest

There are no conflicts to declare.

Data availability

This study is based on previously published data, which are cited in the article. No new data were generated or analyzed.

Acknowledgements

This research is supported by the Postdoctoral Research Special Fund of the International Innovation Institute, Beihang University (2025BKZ105), the National Natural Science Foundation (22341301 and 22595424), the Beijing Natural Science Foundation (L244035), and the Fundamental Research Funds for the Central Universities (501RCQD2025158004).

References

1 C. Yang and Z. Suo, Hydrogel ionotronics, *Nat. Rev. Mater.*, 2018, **3**, 125–142.
2 R. Claes, S. Poncé, G.-M. Rignanese and G. Hautier, Phonon-limited electronic transport through first principles, *Nat. Rev. Phys.*, 2025, **7**, 73–90.
3 K. Feng, *et al.*, Non-fullerene electron-transporting materials for high-performance and stable perovskite solar cells, *Nat. Mater.*, 2025, 1–8.
4 M. Wang, *et al.*, Fusing Stretchable Sensing Technology with Machine Learning for Human–Machine Interfaces, *Adv. Funct. Mater.*, 2021, 2008807.
5 Z. Wang, S. Li and G. Shen, Advanced Sensory Hardware for Intelligent Eye-Machine Interfacing: from Wearables to Bionics, *Adv. Funct. Mater.*, 2025, 2503519.
6 H. Chun and T. D. Chung, Iontronics, *Annu. Rev. Anal. Chem.*, 2015, **8**, 441–462.
7 M. Malakoutian, *et al.*, Lossless Phonon Transition Through GaN-Diamond and Si-Diamond Interfaces, *Adv. Electron. Mater.*, 2025, **11**, 2400146.
8 F. Sun, Q. Lu, S. Feng and T. Zhang, Flexible Artificial Sensory Systems Based on Neuromorphic Devices, *ACS Nano*, 2021, **15**(3), 3875–3899.
9 Z. Wang, *et al.*, A transcription factor-based bacterial biosensor system and its application for on-site detection of explosives, *Biosens. Bioelectron.*, 2024, **244**, 115805.
10 J. Wu, H. Liu, W. Chen, B. Ma and H. Ju, Device integration of electrochemical biosensors, *Nat. Rev. Bioeng.*, 2023, **1**, 346–360.
11 X. Wang, J. Zhou and H. Wang, Bioreceptors as the key components for electrochemical biosensing in medicine, *Cell Rep. Phys. Sci.*, 2024, **5**(2), 101801.
12 K. Wang, *et al.*, Ligand-Responsive Artificial Protein–Protein Communication for Field-Deployable Cell-Free Biosensing, *Angew. Chem.*, 2025, **137**, e202416671.
13 M. Wang, *et al.*, Gesture recognition using a bioinspired learning architecture that integrates visual data with

somatosensory data from stretchable sensors, *Nat. Electron.*, 2020, **3**, 563–570.
14 M. Mahmood, *et al.*, Fully portable and wireless universal brain–machine interfaces enabled by flexible scalp electronics and deep learning algorithm, *Nat. Mach. Intell.*, 2019, **1**, 412–422.
15 Y.-T. Kwon, *et al.*, All-printed nanomembrane wireless bioelectronics using a biocompatible solderable graphene for multimodal human-machine interfaces, *Nat. Commun.*, 2020, **11**, 1–11.
16 S. Sundaram, *et al.*, Learning the signatures of the human grasp using a scalable tactile glove, *Nature*, 2019, **569**, 698–702.
17 B. C.-K. Tee, *et al.*, A skin-inspired organic digital mechanoreceptor, *Science*, 2015, **350**, 313–316.
18 Y. Kim, *et al.*, A bioinspired flexible organic artificial afferent nerve, *Science*, 2018, **360**, 998–1003.
19 C. Wan, *et al.*, An artificial sensory neuron with tactile perceptual learning, *Adv. Mater.*, 2018, **30**, 1801291.
20 Y. H. Jung, B. Park, J. U. Kim and T. I. Kim, Bioinspired electronics for artificial sensory systems, *Adv. Mater.*, 2019, **31**, 1803637.
21 P. Qi, J. Xie, G. Xia, Y. Wang and J. H. Xin, Advanced bionic textile materials: From principles to functional applications, *Adv. Mater.*, 2025, **37**, e02118.
22 H. Niu, *et al.*, Intelligent Robotic Sensory System with Epidermis-Dermis Bionic Electronic Skin for Autonomous Hardness/Softness-Based Material Perception, *Adv. Funct. Mater.*, 2025, 2500511.
23 Z. Liu, *et al.*, A three-dimensionally architected electronic skin mimicking human mechanosensation, *Science*, 2024, **384**, 987–994.
24 X. Meng, *et al.*, A continuous pressure positioning sensor with flexible multilayer structures based on a combinatorial bionic strategy, *Adv. Funct. Mater.*, 2024, **34**, 2314479.
25 W. Wang, *et al.*, Imperceptible augmentation of living systems with organic bioelectronic fibres, *Nat. Electron.*, 2024, **7**, 586–597.
26 S. Shi, *et al.*, A bionic skin for health management: excellent breathability, in situ sensing, and big data analysis, *Adv. Mater.*, 2024, **36**, 2306435.
27 Y. Xu, *et al.*, Bionic e-skin with precise multi-directional droplet sliding sensing for enhanced robotic perception, *Nat. Commun.*, 2024, **15**, 6022.
28 H. Gao, *et al.*, Bio-inspired mid-infrared neuromorphic transistors for dynamic trajectory perception using PdSe2/pentacene heterostructure, *Nat. Commun.*, 2025, **16**, 5241.
29 Y. Hu, *et al.*, Phyto-inspired sustainable and high-performance fabric generators via moisture absorption-evaporation cycles, *Sci. Adv.*, 2024, **10**, eadk4620.
30 Y. Zhang, *et al.*, Adaptive All-Fiber Actuator for Human–Environment Interaction, *ACS Nano*, 2025, **19**, 10232–10243.
31 H. Yuk, B. Lu and X. Zhao, Hydrogel bioelectronics, *Chem. Soc. Rev.*, 2019, **48**, 1642–1667.
32 N. Chen, *et al.*, A photosynthesis-derived bionic system for sustainable biosynthesis, *Angew. Chem.*, 2025, **137**, e202414981.
33 L. Gao, *et al.*, Multilayer Bionic Tunable Strain Sensor with Mutually Non-Interfering Conductive Networks for Machine Learning-Assisted Gesture Recognition, *Adv. Funct. Mater.*, 2025, **35**, 2416911.
34 X. He, *et al.*, Extreme hydrogel bioelectronics, *Adv. Funct. Mater.*, 2024, **34**, 2405896.
35 E. Gouaux and R. MacKinnon, Principles of selective ion transport in channels and pumps, *Science*, 2005, **310**, 1461–1465.
36 T. Yan and J. Liu, Transmembrane ion channels: from natural to artificial systems, *Angew. Chem., Int. Ed.*, 2025, **64**, e202416200.
37 Y. Yuan, Q. Zhang, S. Lin and J. Li, Water: The soul of hydrogels, *Prog. Mater. Sci.*, 2025, **148**, 101378.
38 X. Shi, *et al.*, Phase transition driven tough hydrogel ionic thermoelectric cell with giant thermopower, *Nat. Commun.*, 2025, **16**, 9002.
39 J. Wu, *et al.*, A Biomimetic Ionic Hydrogel Synapse for Self-Powered Tactile-Visual Fusion Perception, *Adv. Funct. Mater.*, 2025, 2500048.
40 Y. Sun, G. Tian, W. Deng and W. Yang, Ionic Hydrogel Sensors Toward Next-Gen Personalized Healthcare, *Adv. Mater.*, 2025, e09122.
41 Y. Lee, W. Song and J.-Y. Sun, Hydrogel soft robotics, *Mater. Today Phys.*, 2020, **15**, 100258.
42 Z. Feng, *et al.*, Flexible intelligent thermal management systems: Sensing devices, signals, and applications, *Nano Energy*, 2025, 110842.
43 C. Keplinger, *et al.*, Stretchable, transparent, ionic conductors, *Science*, 2013, **341**, 984–987.
44 W. Xie, *et al.*, Nonaromatic Persistent Room-Temperature Phosphorescent Hydrogels with Shape Memory Behavior and Ultrahigh Elastic Moduli Based on Partially Hydrolyzed Polyacrylonitrile, *Adv. Funct. Mater.*, 2025, 2504411.
45 J.-Y. Sun, *et al.*, Highly stretchable and tough hydrogels, *Nature*, 2012, **489**, 133–136.
46 C. Larson, *et al.*, Highly stretchable electroluminescent skin for optical signaling and tactile sensing, *Science*, 2016, **351**, 1071–1074.
47 Z. Wu, *et al.*, A wearable ionic hydrogel strain sensor with double cross-linked network for human–machine interface, *Adv. Compos. Hybrid Mater.*, 2025, **8**, 17.
48 Y. Jiang, *et al.*, Strong and ultra-tough ionic hydrogel based on hyperbranched macro-cross-linker: influence of topological structure on properties, *Angew. Chem.*, 2023, **135**, e202310832.
49 X. Liu, J. Liu, S. Lin and X. Zhao, Hydrogel machines, *Mater. Today*, 2020, **36**, 102–104.
50 M. Zhang, *et al.*, Hydrogel muscles powering reconfigurable micro-metastructures with wide-spectrum programmability, *Nat. Mater.*, 2023, **22**, 1243–1252.
51 O. J. Cayre, S. T. Chang and O. D. Velev, Polyelectrolyte diode: nonlinear current response of a junction between

aqueous ionic gels, *J. Am. Chem. Soc.*, 2007, **129**, 10801–10806.
52 K. Xiao, C. Wan, L. Jiang, X. Chen and M. Antonietti, Bioinspired ionic sensory systems: the successor of electronics, *Adv. Mater.*, 2020, **32**, 2000218.
53 K. Xu, Nonaqueous liquid electrolytes for lithium-based rechargeable batteries, *Chem. Rev.*, 2004, **104**, 4303–4418.
54 C.-H. Yim, J. Tam, H. Soboleski and Y. Abu-Lebdeh, On the Correlation between Free Volume, Phase Diagram and Ionic Conductivity of Aqueous and Non-Aqueous Lithium Battery Electrolyte Solutions over a Wide Concentration Range, *J. Electrochem. Soc.*, 2017, **164**, A1002.
55 H. Ma, *et al.*, Biomimetic and biodegradable separator with high modulus and large ionic conductivity enables dendrite-free zinc-ion batteries, *Nat. Commun.*, 2025, **16**, 1014.
56 C. Li, X. Xie, S. Liang and J. Zhou, Issues and future perspective on zinc metal anode for rechargeable aqueous zinc-ion batteries, *Energy Environ. Mater.*, 2020, **3**, 146–159.
57 Q. Wen, *et al.*, Recent advances in interfacial modification of zinc anode for aqueous rechargeable zinc ion batteries, *J. Energy Chem.*, 2023, **83**, 287–303.
58 Y. Guo, *et al.*, Hydrogels and hydrogel-derived materials for energy and water sustainability, *Chem. Rev.*, 2020, **120**, 7642–7707.
59 D. N. Ampong, *et al.*, Harnessing hydrogels for electrochemical energy and environmental sustainability, *Renewable Sustainable Energy Rev.*, 2026, **229**, 116628.
60 H. Wu, *et al.*, The effects of electrolyte on the supercapacitive performance of activated calcium carbide-derived carbon, *J. Power Sources*, 2013, **226**, 202–209.
61 N. Zhang, *et al.*, Cation-deficient spinel ZnMn2O4 cathode in Zn (CF3SO3) 2 electrolyte for rechargeable aqueous Zn-ion battery, *J. Am. Chem. Soc.*, 2016, **138**, 12894–12901.
62 X. Zhou, F. Zhao, Y. Guo, B. Rosenberger and G. Yu, Architecting highly hydratable polymer networks to tune the water state for solar water purification, *Sci. Adv.*, 2019, **5**, eaaw5484.
63 Y. Sekine and T. Ikeda-Fukazawa, Structural changes of water in a hydrogel during dehydration, *J. Chem. Phys.*, 2009, **130**(3), 034501.
64 K. Wang, *et al.*, Chemically crosslinked hydrogel film leads to integrated flexible supercapacitors with superior performance, *Adv. Mater.*, 2015, **27**, 7451–7457.
65 C. Tang, *et al.*, A new polyvinyl alcohol lithium chloride hydrogel electrolyte: high ionic conductivity and wide working temperature range, *Adv. Funct. Mater.*, 2025, **35**, 2417207.
66 S. Kondou, *et al.*, Poly (ionic liquid) electrolytes at an extreme salt concentration for solid-state batteries, *J. Am. Chem. Soc.*, 2024, **146**, 33169–33178.
67 D. Wang, *et al.*, A Nanofibrillated Cellulose/Polyacrylamide Electrolyte-Based Flexible and Sewable High-Performance Zn–MnO2 Battery with Superior Shear Resistance, *Small*, 2018, **14**, 1803978.
68 Y. Zhou, *et al.*, Highly stretchable, elastic, and ionic conductive hydrogel for artificial soft electronics, *Adv. Funct. Mater.*, 2019, **29**, 1806220.
69 E. C. Lloyd, *et al.*, Porous hierarchically ordered hydrogels demonstrating structurally dependent mechanical properties, *Nat. Commun.*, 2025, **16**, 3792.
70 F. Zhang, *et al.*, Flexible dry hydrogel with lamella-like structure engineered via dehydration in poor solvent, *CCS Chem.*, 2020, **2**, 533–543.
71 X. Peng, *et al.*, A zwitterionic gel electrolyte for efficient solid-state supercapacitors, *Nat. Commun.*, 2016, **7**, 1–8.
72 J. Yang, *et al.*, Antifreezing Zwitterionic Hydrogel Electrolyte with High Conductivity of 12.6 mS cm− 1 at− 40 °C through Hydrated Lithium Ion Hopping Migration, *Adv. Funct. Mater.*, 2021, 2009438.
73 D. Fu, Y. Lu, Z. Peng and W. Zhong, A zwitterionic hydrogel with a surprising function of increasing the ionic conductivity of alkali metal chloride or sulfuric acid water-soluble electrolyte, *J. Mater. Chem. A*, 2023, **11**, 13543–13551.
74 C. Tiyapiboonchaiya, *et al.*, The zwitterion effect in high-conductivity polyelectrolyte materials, *Nat. Mater.*, 2004, **3**, 29–32.
75 F. Mo, *et al.*, Zwitterionic Sulfobetaine Hydrogel Electrolyte Building Separated Positive/Negative Ion Migration Channels for Aqueous Zn-MnO2 Batteries with Superior Rate Capabilities, *Adv. Energy Mater.*, 2020, **10**, 2000035.
76 Y. Xu, *et al.*, Self-adhesive polyzwitterionic hydrogel electrolytes for long-life flexible zinc-ion batteries, *J. Mater. Chem. A*, 2024, **12**, 13191–13202.
77 J. Yeom, *et al.*, Soft and ion-conducting hydrogel artificial tongue for astringency perception, *Sci. Adv.*, 2020, **6**, eaba5785.
78 H. O. Ford, B. Park, J. Jiang, M. E. Seidler and J. L. Schaefer, Enhanced Li+ Conduction within Single-Ion Conducting Polymer Gel Electrolytes via Reduced Cation–Polymer Interaction, *ACS Mater. Lett.*, 2020, **2**, 272–279.
79 Z. Li, *et al.*, Ionic conduction in polymer-based solid electrolytes, *Adv. Sci.*, 2023, **10**, 2201718.
80 Q. Zhang, T. Bian, X. Wang, R. Shi and Y. Zhao, Unlocking mechanism of anion and cation interaction on ion conduction of polymer based electrolyte in metal batteries, *Angew. Chem., Int. Ed.*, 2025, **64**, e202415343.
81 K. M. Diederichsen, H. G. Buss and B. D. McCloskey, The compensation effect in the Vogel–Tammann–Fulcher (VTF) equation for polymer-based electrolytes, *Macromolecules*, 2017, **50**, 3831–3840.
82 D. G. Mackanic, *et al.*, Decoupling of mechanical properties and ionic conductivity in supramolecular lithium ion conductors, *Nat. Commun.*, 2019, **10**, 1–11.
83 G. Wang, T. Zhang, L. Hu, K. Shi and X. Yu, Engineering crystalline property of polymer solid electrolytes for boosted electrochemical performances: a critical review, *J. Mater. Chem. A*, 2025, **13**, 26880–26898.
84 J. Petry, M. Dietel and M. Thelakkat, Semi-Interpenetrating Network Electrolytes Utilizing Ester-Functionalized Low Tg

Polysiloxanes in Lithium-Metal Batteries, *Adv. Energy Mater.*, 2025, **15**, 2403531.
85 G. Wu, S. Lin and C. Yang, Preparation and characterization of PVA/PAA membranes for solid polymer electrolytes, *J. Membr. Sci.*, 2006, **275**, 127–133.
86 Z. Song, *et al.*, A rechargeable Zn–air battery with high energy efficiency and long life enabled by a highly water-retentive gel electrolyte with reaction modifier, *Adv. Mater.*, 2020, **32**, 1908127.
87 J. Fu, *et al.*, A flexible solid-state electrolyte for wide-scale integration of rechargeable zinc–air batteries, *Energy Environ. Sci.*, 2016, **9**, 663–670.
88 Y. Tanaka, *et al.*, New oxyhalide solid electrolytes with high lithium ionic conductivity> 10 mS cm− 1 for all-solid-state batteries, *Angew. Chem., Int. Ed.*, 2023, **62**, e202217581.
89 Z. Du, *et al.*, A Robust and Tough Composite Hydrogel Electrolyte with Anion-Locked Supramolecular Network for Zinc Ion Batteries, *Adv. Mater.*, 2025, 2502328.
90 D. Buenger, F. Topuz and J. Groll, Hydrogels in sensing applications, *Prog. Polym. Sci.*, 2012, **37**, 1678–1719.
91 T. Wan, *et al.*, In-sensor computing: materials, devices, and integration technologies, *Adv. Mater.*, 2023, **35**, 2203830.
92 S. Y. Zhuo, C. Song, Q. F. Rong, T. Y. Zhao and M. J. Liu, Shape and stiffness memory ionogels with programmable pressure-resistance response, *Nat. Commun.*, 2022, **13**(1), 1743.
93 P. Cui, *et al.*, Liquid Metal-Reinfored Hierarchically Aligned Double-Network Hydrogels: Ultrahigh Crack/Fatigue Resistance and Strain-Responsive Sensing, *Small*, 2026, e12709.
94 X. Pu, *et al.*, Ultrastretchable, transparent triboelectric nanogenerator as electronic skin for biomechanical energy harvesting and tactile sensing, *Sci. Adv.*, 2017, **3**, e1700015.
95 H. Wang, *et al.*, Biomass-based dual-network multifunctional hydrogel for durable wearable sensors and emergency hemostasis, *Chem. Eng. J.*, 2026, 172777.
96 W. Y. Chen, X. Jiang, S.-N. Lai, D. Peroulis and L. Stanciu, Nanohybrids of a MXene and transition metal dichalcogenide for selective detection of volatile organic compounds, *Nat. Commun.*, 2020, **11**, 1302.
97 H. Yang, *et al.*, Wireless Ti3C2T x MXene strain sensor with ultrahigh sensitivity and designated working windows for soft exoskeletons, *ACS Nano*, 2020, **14**, 11860–11875.
98 Q. Tian, W. Yan, Y. Li and D. Ho, Bean pod-inspired ultrasensitive and self-healing pressure sensor based on laser-induced graphene and polystyrene microsphere sandwiched structure, *ACS Appl. Mater. Interfaces*, 2020, **12**, 9710–9717.
99 S. Gandla, *et al.*, Highly linear and stable flexible temperature sensors based on laser-induced carbonization of polyimide substrates for personal mobile monitoring, *Adv. Mater. Technol.*, 2020, **5**, 2000014.
100 J. Chen, *et al.*, Superelastic, sensitive, and low hysteresis flexible strain sensor based on wave-patterned liquid metal for human activity monitoring, *ACS Appl. Mater. Interfaces*, 2020, **12**, 22200–22211.
101 J. C. Yeo, *et al.*, Triple-state liquid-based microfluidic tactile sensor with high flexibility, durability, and sensitivity, *ACS Sens.*, 2016, **1**, 543–551.
102 Y. Zhang, *et al.*, Highly stretchable and sensitive pressure sensor array based on icicle-shaped liquid metal film electrodes, *ACS Appl. Mater. Interfaces*, 2020, **12**, 27961–27970.
103 B. Yao, *et al.*, Stretchable strain sensors based on liquid metal channels with simultaneous significant improvements in linearity and sensitivity, *Adv. Funct. Mater.*, 2026, **36**, e17648.
104 J. Wu, *et al.*, Extremely deformable, transparent, and high-performance gas sensor based on ionic conductive hydrogel, *ACS Appl. Mater. Interfaces*, 2018, **11**, 2364–2373.
105 J. Wu, *et al.*, An intrinsically stretchable humidity sensor based on anti-drying, self-healing and transparent organohydrogels, *Mater. Horiz.*, 2019, **6**, 595–603.
106 Z. Lei and P. Wu, A highly transparent and ultra-stretchable conductor with stable conductivity during large deformation, *Nat. Commun.*, 2019, **10**, 3429.
107 R. Priyadarshi, Energy-Efficient Routing in Wireless Sensor Networks: A Meta-heuristic and Artificial Intelligence-based Approach: A Comprehensive Review, *Arch. Comput. Methods Eng.*, 2024, **31**(4), 2109–2137.
108 H. Ota, *et al.*, Highly deformable liquid-state heterojunction sensors, *Nat. Commun.*, 2014, **5**, 1–9.
109 Z. Lei and P. Wu, A highly transparent and ultra-stretchable conductor with stable conductivity during large deformation, *Nat. Commun.*, 2019, **10**, 1–9.
110 Z. Wu, *et al.*, Ultrasensitive, Stretchable, and Fast-Response Temperature Sensors Based on Hydrogel Films for Wearable Applications, *ACS Appl. Mater. Interfaces*, 2021, **13**(18), 21854–21864.
111 Z. Lei and P. Wu, A supramolecular biomimetic skin combining a wide spectrum of mechanical properties and multiple sensory capabilities, *Nat. Commun.*, 2018, **9**, 1134.
112 J. Wu, *et al.*, Ultrasensitive and stretchable temperature sensors based on thermally stable and self-healing organohydrogels, *ACS Appl. Mater. Interfaces*, 2020, **12**, 19069–19079.
113 Z. Wu, X. Yang and J. Wu, Conductive hydrogel-and organohydrogel-based stretchable sensors, *ACS Appl. Mater. Interfaces*, 2021, **13**, 2128–2144.
114 Z. Lei, Q. Wang and P. Wu, A multifunctional skin-like sensor based on a 3D printed thermo-responsive hydrogel, *Mater. Horiz.*, 2017, **4**, 694–700.
115 E. Karimi-Sibaki, A. Kharicha, M. Wu, A. Ludwig and J. Bohacek, Confrontation of the Ohmic approach with the ionic transport approach for modeling the electrical behavior of an electrolyte, *Ionics*, 2018, **24**, 2157–2165.
116 Z. Zhang, C. Li, J. Zhang, M. Eikerling and J. Huang, Dynamic response of ion transport in nanoconfined electrolytes, *Nano Lett.*, 2023, **23**, 10703–10709.

117 P. Faeghifard, M. Mehranpour and I. Ghasemi, Fabrication and Investigation on Mechanical, Electrical, and Sensing Performance of Polydimethylsiloxane/Carbon Nanotube and Thermoplastic Polyurethane/Carbon Nanotube Wearable Strain Sensors, *Adv. Eng. Mater.*, 2025, **27**, 2402208.
118 S. Cheng, Y. S. Narang, C. Yang, Z. Suo and R. D. Howe, Stick-on large-strain sensors for soft robots, *Adv. Mater. Interfaces*, 2019, **6**, 1900985.
119 Q. Rong, *et al.*, Anti-freezing, conductive self-healing organohydrogels with stable strain-sensitivity at subzero temperatures, *Angew. Chem., Int. Ed.*, 2017, **56**, 14159–14163.
120 Z. G. Zhao, *et al.*, Bicontinuous vitrimer heterogels with wide-span switchable stiffness-gated iontronic coordination, *Sci. Adv.*, 2024, **10**(10), eadl2737.
121 D. Mostaghniyazdi and S. E. Nodehi, Resistive Sensing in Soft Robotic Grippers: A Comprehensive Review of Strain, Tactile, and Ionic Sensors, *Electronics*, 2025, **14**, 4290.
122 X. Cui, Y. Xi, S. Tu and Y. Zhu, An overview of flexible sensors from ionic liquid-based gels, *TrAC, Trends Anal. Chem.*, 2024, **174**, 117662.
123 H. Qiao, *et al.*, A highly sensitive and flexible capacitive pressure sensor based on an ionic hydrogel dielectric layer with a lateral-bending microstructure, *J. Mater. Chem. C*, 2024, **12**, 13485–13494.
124 Z. Zhao, *et al.*, Recent development of self-powered tactile sensors based on ionic hydrogels, *Gels*, 2023, **9**, 257.
125 F. Zhuo, *et al.*, Advanced Morphological and Material Engineering for High-Performance Interfacial Iontronic Pressure Sensors, *Adv. Sci.*, 2025, **12**, 2413141.
126 N. Unsuree, *et al.*, A review: ion transport of two-dimensional materials in novel technologies from macro to nanoscopic perspectives, *Energies*, 2021, **14**, 5819.
127 Z. Cao, *et al.*, A programmable electronic skin with event-driven in-sensor touch differential and decision-making, *Adv. Funct. Mater.*, 2025, **35**, 2412649.
128 C.-C. Kim, H.-H. Lee, K. H. Oh and J.-Y. Sun, Highly stretchable, transparent ionic touch panel, *Science*, 2016, **353**, 682–687.
129 G. Gao, *et al.*, Bioinspired Self-Healing Human–Machine Interactive Touch Pad with Pressure-Sensitive Adhesiveness on Targeted Substrates, *Adv. Mater.*, 2020, **32**, 2004290.
130 Y. Li, *et al.*, An ultrastretchable and multifunctional hydrophobic/electrostatic dual-crosslinked hydrogel for self-healing flexible touch panel and sensor, *npj Flexible Electron.*, 2025, **9**, 45.
131 Z. Zhao, *et al.*, Freestanding flag-type triboelectric nanogenerator for harvesting high-altitude wind energy from arbitrary directions, *ACS Nano*, 2016, **10**, 1780–1787.
132 X. Pu, *et al.*, Wearable self-charging power textile based on flexible yarn supercapacitors and fabric nanogenerators, *Adv. Mater.*, 2016, **28**, 98–105.
133 S. Niu and Z. L. Wang, Theoretical systems of triboelectric nanogenerators, *Nano Energy*, 2015, **14**, 161–192.
134 D. Tao, *et al.*, Electro-spun nanofibers-based triboelectric nanogenerators in wearable electronics: status and perspectives, *npj Flexible Electron.*, 2025, **9**, 4.
135 Ankit, N. Tiwari, M. Rajput, N. A. Chien and N. Mathews, Highly transparent and integrable surface texture change device for localized tactile feedback, *Small*, 2018, **14**, 1702312.
136 M. S. Sarwar, *et al.*, Bend, stretch, and touch: Locating a finger on an actively deformed transparent sensor array, *Sci. Adv.*, 2017, **3**, e1602200.
137 Y. Lee, *et al.*, Ionic spiderwebs, *Sci. Rob.*, 2020, **5**, eaaz5405.
138 J. Shi, S. Xie, Z. Liu, M. Cai and C. F. Guo, Non-hygroscopic ionogel-based humidity-insensitive iontronic sensor arrays for intra-articular pressure sensing, *Nat. Sci. Rev.*, 2024, **11**, nwae351.
139 S. Roubert Martinez, P. Le Floch, J. Liu and R. D. Howe, Pure Conducting Polymer Hydrogels Increase Signal-to-Noise of Cutaneous Electrodes by Lowering Skin Interface Impedance, *Adv. Healthcare Mater.*, 2023, **12**, 2202661.
140 Z. Li, *et al.*, Ultrafast readout, crosstalk suppression iontronic array enabled by frequency-coding architecture, *NPJ Flexible Electron.*, 2024, **8**, 9.
141 C. H. Yang, *et al.*, Ionic cable, *Extreme Mech. Lett.*, 2015, **3**, 59–65.
142 C. Duan, W. Wang and Q. Xie, Fabrication of nanofluidic devices, *Biomicrofluidics*, 2013, **7**, 026501.
143 X. Wei, *et al.*, Covalent organic framework membrane with hourglass-shaped nanochannels for ultrafast desalination, *Nat. Commun.*, 2025, **16**, 8125.
144 R. M. Wen, *et al.*, Designing Confined Thermal-Recognized Hydrogen Bonding Nanochannels for Effective and Energy-Efficient Water Isotopologue Sieving, *Adv. Funct. Mater.*, 2025, **35**, 2423564.
145 J. Huang, X. Pan and N. Yan, Structural biology and molecular pharmacology of voltage-gated ion channels, *Nat. Rev. Mol. Cell Biol.*, 2024, **25**, 904–925.
146 H. Daiguji, P. Yang and A. Majumdar, Ion transport in nanofluidic channels, *Nano Lett.*, 2004, **4**, 137–142.
147 W. Kong, *et al.*, Strong, Water-Stable Ionic Cable from Bio-Hydrogel, *Chem. Mater.*, 2019, **31**, 9288–9294.
148 G. Chen, *et al.*, A highly conductive cationic wood membrane, *Adv. Funct. Mater.*, 2019, **29**, 1902772.
149 W. Kong, *et al.*, Muscle-Inspired Highly Anisotropic, Strong, Ion-Conductive Hydrogels, *Adv. Mater.*, 2018, **30**, 1801934.
150 Y.-C. Lin, H.-H. Chen, C.-W. Chu and L.-H. Yeh, Massively enhanced charge selectivity, ion transport, and osmotic energy conversion by antiswelling nanoconfined hydrogels, *Nano Lett.*, 2024, **24**, 11756–11762.
151 F. Lin, *et al.*, Muscle-Inspired Robust Anisotropic Cellulose Conductive Hydrogel for Multidirectional Strain Sensors and Implantable Bioelectronics, *Adv. Funct. Mater.*, 2025, **35**, 2416419.
152 G. Buzsáki, C. A. Anastassiou and C. Koch, The origin of extracellular fields and currents—EEG, ECoG, LFP and spikes, *Nat. Rev. Neurosci.*, 2012, **13**, 407–420.
153 J. Tu, *et al.*, Wearable biomolecular sensing nanotechnologies in chronic disease management, *Nat. Nanotechnol.*, 2025, 1–17.

154 N. A. Alba, R. J. Sclabassi, M. Sun and X. T. Cui, Novel hydrogel-based preparation-free EEG electrode, *IEEE Trans. Neural Syst. Rehabil. Eng.*, 2010, **18**, 415–423.
155 D. Boufidis, R. Garg, E. Angelopoulos, D. K. Cullen and F. Vitale, Bio-inspired electronics: Soft, biohybrid, and "living" neural interfaces, *Nat. Commun.*, 2025, **16**, 1861.
156 P. Moshayedi, *et al.*, The relationship between glial cell mechanosensitivity and foreign body reactions in the central nervous system, *Biomaterials*, 2014, **35**, 3919–3925.
157 J. O. Winter, S. F. Cogan and J. F. Rizzo III, Neurotrophin-eluting hydrogel coatings for neural stimulating electrodes, *J. Biomed. Mater. Res., Part B*, 2007, **81**, 551–563.
158 S. Zhao, *et al.*, Programmable hydrogel ionic circuits for biologically matched electronic interfaces, *Adv. Mater.*, 2018, **30**, 1800598.
159 H. Yoon, *et al.*, Decoding tissue biomechanics using conformable electronic devices, *Nat. Rev. Mater.*, 2025, **10**, 4–27.
160 S. Zhuo, *et al.*, Reusable free-standing hydrogel electronic tattoo sensors with superior performance, *NPJ Flexible Electron.*, 2024, **8**(1), 49, DOI: **10.1038/s41528-024-00335-x.**
161 S. H. Kim, *et al.*, Ultrastretchable conductor fabricated on skin-like hydrogel–elastomer hybrid substrates for skin electronics, *Adv. Mater.*, 2018, **30**, 1800109.
162 K. Nagamine, S. Chihara, H. Kai, H. Kaji and M. Nishizawa, Totally shape-conformable electrode/hydrogel composite for on-skin electrophysiological measurements, *Sens. Actuators, B*, 2016, **237**, 49–53.
163 Y. Lu, *et al.*, Stretchable graphene–hydrogel interfaces for wearable and implantable bioelectronics, *Nat. Electron.*, 2024, **7**, 51–65.
164 B. Cui, *et al.*, Bio-Inspired Self-Renewing Implant Surfaces With Sequential Biofunctional Adaptation for Infectious Diabetic Tissue Repair, *Adv. Funct. Mater.*, 2025, **35**, 2418092.
165 H. Sheng, *et al.*, Neural interfaces by hydrogels, *Extreme Mech. Lett.*, 2019, **30**, 100510.
166 H. Yoo, Y. H. Lee, M.-G. Lee and J.-Y. Sun, Gel-Based Ionic Circuits, *Chem. Rev.*, 2025, **125**, 8956–9011.
167 H. Li, *et al.*, CMOS electrochemical instrumentation for biosensor microsystems: A review, *Sensors*, 2016, **17**, 74.
168 S. Cohen-Cory, The developing synapse: construction and modulation of synaptic structures and circuits, *Science*, 2002, **298**, 770–776.
169 Y. Wu, D. Wang, I. Willner, Y. Tian and L. Jiang, Smart DNA hydrogel integrated nanochannels with high ion flux and adjustable selective ionic transport, *Angew. Chem., Int. Ed.*, 2018, **57**, 7790–7794.
170 Y. Wang, Z. Wang, Z. Su and S. Cai, Stretchable and transparent ionic diode and logic gates, *Extreme Mech. Lett.*, 2019, **28**, 81–86.
171 K. Tybrandt, E. O. Gabrielsson and M. Berggren, Toward complementary ionic circuits: The npn ion bipolar junction transistor, *J. Am. Chem. Soc.*, 2011, **133**, 10141–10145.
172 K. Tybrandt, K. C. Larsson, A. Richter-Dahlfors and M. Berggren, Ion bipolar junction transistors, *Proc. Natl. Acad. Sci. U. S. A.*, 2010, **107**, 9929–9932.
173 Z. Zhang, B. Sabbagh, Y. Chen and G. Yossifon, Geometrically scalable iontronic memristors: Employing bipolar polyelectrolyte gels for neuromorphic systems, *ACS Nano*, 2024, **18**, 15025–15034.
174 H. J. Koo, J. H. So, M. D. Dickey and O. D. Velev, Towards all-soft matter circuits: prototypes of quasi-liquid devices with memristor characteristics, *Adv. Mater.*, 2011, **23**, 3559–3564.
175 J. H. Han, K. B. Kim, H. C. Kim and T. D. Chung, Ionic circuits based on polyelectrolyte diodes on a microchip, *Angew. Chem., Int. Ed.*, 2009, **48**, 3830–3833.
176 C. C. Harrell, P. Kohli, Z. Siwy and C. R. Martin, DNA–nanotube artificial ion channels, *J. Am. Chem. Soc.*, 2004, **126**, 15646–15647.
177 I. Vlassiouk and Z. S. Siwy, Nanofluidic diode, *Nano Lett.*, 2007, **7**, 552–556.
178 X. Zhang, *et al.*, DNA-Functionalized Solid-State Nanochannels with Enhanced Sensing, *Acc. Mater. Res.*, 2024, **6**, 285–293.
179 Z. Zheng, D. J. Hansford and A. T. Conlisk, Effect of multivalent ions on electroosmotic flow in micro-and nanochannels, *Electrophoresis*, 2003, **24**, 3006–3017.
180 H. Chun, T. D. Chung and H. C. Kim, Cytometry and velocimetry on a microfluidic chip using polyelectrolytic salt bridges, *Anal. Chem.*, 2005, **77**, 2490–2495.
181 S.-M. Lim, *et al.*, Ion-to-ion amplification through an open-junction ionic diode, *Proc. Natl. Acad. Sci. U. S. A.*, 2019, **116**, 13807–13815.
182 H. Yoo, *et al.*, G-Quadruplex-Filtered Selective Ion-to-Ion Current Amplification for Non-Invasive Ion Monitoring in Real Time, *Adv. Mater.*, 2023, **35**, 2303655.
183 H. R. Lee, *et al.*, A stretchable ionic diode from copolyelectrolyte hydrogels with methacrylated polysaccharides, *Adv. Funct. Mater.*, 2019, **29**, 1806909.
184 P. Xu, X. Wu, Z. Zhang, P. Pan and X. Liu, Enhancing the rectification effect of hydrogel-based stretchable ionic diodes through incorporating cations with high valence, *Microsyst. Nanoeng.*, 2025, **11**, 139.
185 F. Jiang, *et al.*, Ion rectification based on gel polymer electrolyte ionic diode, *Nat. Commun.*, 2022, **13**, 6669.
186 L. Ma, *et al.*, Modulation of ionic current rectification in ultrashort conical nanopores, *Anal. Chem.*, 2020, **92**, 16188–16196.
187 C.-H. Chiang, *et al.*, Single symmetric nanopores in ultrathin crystalline ferroelectric BiFeO3 as polarization-switchable ionic diodes, *Nat. Commun.*, 2026, **17**, 1542.
188 K. B. Kim, J.-H. Han, H. C. Kim and T. D. Chung, Polyelectrolyte junction field effect transistor based on microfluidic chip, *Appl. Phys. Lett.*, 2010, **96**(14), 143506.
189 Y. He, Y. Zhu and Q. Wan, Oxide ionic neuro-transistors for bio-inspired computing, *Nanomaterials*, 2024, **14**, 584.
190 C. Cheng, M. Z. Rashed and G. Y. Fridman, Ionic transistor using ion exchange membranes, *Lab Chip*, 2022, **22**, 2707–2713.
191 X. Teng, *et al.*, Ion effects on salt-in-water electrolyte gated polymer electrochemical transistors, *Org. Electron.*, 2023, **120**, 106859.

192 R. Waser, R. Dittmann, G. Staikov and K. Szot, Redox-based resistive switching memories–nanoionic mechanisms, prospects, and challenges, *Adv. Mater.*, 2009, **21**, 2632–2663.
193 G. Zhou, *et al.*, Volatile and nonvolatile memristive devices for neuromorphic computing, *Adv. Electron. Mater.*, 2022, **8**, 2101127.
194 J. Borghetti, *et al.*, 'Memristive'switches enable 'stateful'-logic operations via material implication, *Nature*, 2010, **464**, 873–876.
195 B. Chen, *et al.*, Highly stretchable and transparent ionogels as nonvolatile conductors for dielectric elastomer transducers, *ACS Appl. Mater. Interfaces*, 2014, **6**, 7840–7845.
196 T. Li, *et al.*, Fast-moving soft electronic fish, *Sci. Adv.*, 2017, **3**, e1602045.
197 N. Kellaris, V. G. Venkata, G. M. Smith, S. K. Mitchell and C. Keplinger, Peano-HASEL actuators: Muscle-mimetic, electrohydraulic transducers that linearly contract on activation, *Sci. Rob.*, 2018, **3**(14), eaar3276.
198 Y. Osada and J. P. Gong, Soft and wet materials: polymer gels, *Adv. Mater.*, 1998, **10**, 827–837.
199 Y.-W. Kang, J. Woo, H.-R. Lee and J.-Y. Sun, A mechanically enhanced electroactive hydrogel for 3D printing using a multileg long chain crosslinker, *Smart Mater. Struct.*, 2019, **28**, 095016.
200 L. P. Ferraz and E. K. Silva, Pulsed electric field-assisted extraction techniques for obtaining vegetable oils and essential oils: Recent progress and opportunities for the food industry, *Sep. Purif. Technol.*, 2025, **354**, 128833.
201 G. Keiser, Optical fiber communications, *Wiley Encyclopedia of Telecommunications*, 2003.
202 Y. Liu, *et al.*, Super stable, highly ion-conductive and transparent eutecto-/hydro-gel promotes wearable electronic and visual strain sensing, *Chem. Eng. J.*, 2023, **461**, 141965.
203 M. Grätzel, Ultrafast colour displays, *Nature*, 2001, **409**, 575–576.
204 Y. Zhou, *et al.*, Hydrogel smart windows, *J. Mater. Chem. A*, 2020, **8**, 10007–10025.
205 C. H. Yang, S. Zhou, S. Shian, D. R. Clarke and Z. Suo, Organic liquid-crystal devices based on ionic conductors, *Mater. Horiz.*, 2017, **4**, 1102–1109.
206 C. H. Yang, B. Chen, J. Zhou, Y. M. Chen and Z. Suo, Electroluminescence of giant stretchability, *Adv. Mater.*, 2016, **28**, 4480–4484.
207 B. Chen, *et al.*, All-solid ionic eye, *J. Appl. Mech.*, 2021, **88**, 031016.
208 X. Chen, H. Huang, L. Pan, T. Liu and M. Niederberger, Fully integrated design of a stretchable solid-state lithium-ion full battery, *Adv. Mater.*, 2019, **31**, 1904648.
209 L. Zhong, Y. Lu, H. Li, Z. Tao and J. Chen, High-performance aqueous sodium-ion batteries with hydrogel electrolyte and alloxazine/CMK-3 anode, *ACS Sustainable Chem. Eng.*, 2018, **6**, 7761–7768.
210 X. A. Jiang, *et al.*, Physical ionogels with only 2 wt % gelators as efficient quasi-solid-state electrolytes for lithium batteries, *Matter*, 2024, **7**(4), 1558–1574.
211 H. Li, *et al.*, An extremely safe and wearable solid-state zinc ion battery based on a hierarchical structured polymer electrolyte, *Energy Environ. Sci.*, 2018, **11**, 941–951.
212 Y. Huang, *et al.*, Solid-state rechargeable Zn//NiCo and Zn–air batteries with ultralong lifetime and high capacity: the role of a sodium polyacrylate hydrogel electrolyte, *Adv. Energy Mater.*, 2018, **8**, 1802288.
213 Z. Wang, *et al.*, Hydrogel electrolytes for flexible aqueous energy storage devices, *Adv. Funct. Mater.*, 2018, **28**, 1804560.
214 H. Gwon, *et al.*, Recent progress on flexible lithium rechargeable batteries, *Energy Environ. Sci.*, 2014, **7**, 538–551.
215 Y. Huang, *et al.*, Electrolytes and Electrolyte/Electrode Interfaces in Sodium-Ion Batteries: From Scientific Research to Practical Application, *Adv. Mater.*, 2019, **31**, 1808393.
216 Y. Shi, *et al.*, Nanostructured conductive polymer gels as a general framework material to improve electrochemical performance of cathode materials in Li-ion batteries, *Nano Lett.*, 2017, **17**, 1906–1914.
217 M.-C. Lin, *et al.*, An ultrafast rechargeable aluminium-ion battery, *Nature*, 2015, **520**, 324–328.
218 J.-M. McGregor, *et al.*, Organic electrolyte cations promote non-aqueous CO2 reduction by mediating interfacial electric fields, *Nat. Catal.*, 2025, **8**, 79–91.
219 W. Wang, *et al.*, Compensating K Ions Through an Organic Salt in Electrolytes for Practical K-Ion Batteries, *Angew. Chem.*, 2025, **137**, e202424516.
220 H. Li, *et al.*, Advanced rechargeable zinc-based batteries: recent progress and future perspectives, *Nano Energy*, 2019, **62**, 550–587.
221 Y. Wang, *et al.*, Boosting Performance of Quasi-Solid-State Zinc Ion Batteries via Zincophilic Solubilization, *Angew. Chem.*, 2025, **137**, e202508556.
222 L. Li, Z. Wu, S. Yuan and X.-B. Zhang, Advances and challenges for flexible energy storage and conversion devices and systems, *Energy Environ. Sci.*, 2014, **7**, 2101–2122.
223 Y. Xu, *et al.*, Flexible solid-state supercapacitors based on three-dimensional graphene hydrogel films, *ACS Nano*, 2013, **7**, 4042–4049.
224 S. Ghosh and O. Inganäs, Conducting polymer hydrogels as 3D electrodes: applications for supercapacitors, *Adv. Mater.*, 1999, **11**, 1214–1218.
225 Q. Tang, M. Chen, G. Wang, H. Bao and P. Saha, A facile prestrain-stick-release assembly of stretchable supercapacitors based on highly stretchable and sticky hydrogel electrolyte, *J. Power Sources*, 2015, **284**, 400–408.
226 D. G. Mackanic, M. Kao and Z. Bao, Enabling deformable and stretchable batteries, *Adv. Energy Mater.*, 2020, **10**, 2001424.
227 Z. Lv, *et al.*, Editable supercapacitors with customizable stretchability based on mechanically strengthened

ultralong MnO2 nanowire composite, *Adv. Mater.*, 2018, **30**, 1704531.
228 F. Han, *et al.*, Hybrid microstructure-based stretchable biosensors for multi-physiological signal sensing, *EScience*, 2025, **5**, 100327.
229 J. Yang, *et al.*, Electrochemical integrated driven patterning of liquid metal/MXene hydrogel electrodes for stretchable microsupercapacitors, *Energy Storage Mater.*, 2025, 104764.
230 C. R. Chen, H. Qin, H. P. Cong and S. H. Yu, A highly stretchable and real-time healable supercapacitor, *Adv. Mater.*, 2019, **31**, 1900573.
231 S. Huang, *et al.*, A self-healing integrated all-in-one zinc-ion battery, *Angew. Chem.*, 2019, **131**, 4357–4361.
232 K. Fu, *et al.*, Self-healing hydrogels in flexible energy storage devices: mechanisms, applications, and prospects, *J. Mater. Chem. A*, 2026, **14**, 1422–1449.
233 F. Mo, *et al.*, A flexible rechargeable aqueous zinc manganese-dioxide battery working at −20 °C, *Energy Environ. Sci.*, 2019, **12**, 706–715.
234 Q. Rong, W. Lei, J. Huang and M. Liu, Low temperature tolerant organohydrogel electrolytes for flexible solid-state supercapacitors, *Adv. Energy Mater.*, 2018, **8**, 1801967.
235 Z. Pei, *et al.*, Flexible Rechargeable Zinc-Air Battery with Excellent Low-Temperature Adaptability, *Angew. Chem.*, 2020, **59**(12), 4793–4799.
236 Z. Wang, *et al.*, A flexible rechargeable zinc-ion wire-shaped battery with shape memory function, *J. Mater. Chem. A*, 2018, **6**, 8549–8557.
237 L. Liu, *et al.*, Watchband-like supercapacitors with body temperature inducible shape memory ability, *Adv. Energy Mater.*, 2016, **6**, 1600763.
238 F. Mo, *et al.*, A smart safe rechargeable zinc ion battery based on sol-gel transition electrolytes, *Sci. Bull.*, 2018, **63**, 1077–1086.
239 J. Zhao, *et al.*, A smart flexible zinc battery with cooling recovery ability, *Angew. Chem.*, 2017, **129**, 7979–7983.
240 J. Zhu, M. Yao, S. Huang, J. Tian and Z. Niu, Thermal-Gated Polymer Electrolytes for Smart Zinc-Ion Batteries, *Angew. Chem., Int. Ed.*, 2020, **59**, 16480–16484.
241 J. Duan, *et al.*, Tough hydrogel diodes with tunable interfacial adhesion for safe and durable wearable batteries, *Nano Energy*, 2018, **48**, 569–574.
242 J. X. Xu, *et al.*, Sustainable moisture energy, *Nat. Rev. Mater.*, 2024, **9**, 722–737, DOI: **10.1038/s41578-023-00643-0**.
243 Y. Wang, *et al.*, Solvent-Mediated Microphase Separation in Ionogels for the Construction of Mechanically Robust and High-Energy-Output Moisture-Electric Generators, *Interdiscip. Mater.*, 2025, **4**, 869–880, DOI: **10.1002/idm2.70019**.
244 W. Xu, *et al.*, Environmentally friendly hydrogel-based triboelectric nanogenerators for versatile energy harvesting and self-powered sensors, *Adv. Energy Mater.*, 2017, **7**, 1601529.
245 Q. Guan, *et al.*, Highly efficient self-healable and dual responsive hydrogel-based deformable triboelectric nanogenerators for wearable electronics, *J. Mater. Chem. A*, 2019, **7**, 13948–13955.
246 X. Wang, *et al.*, Bioinspired stretchable triboelectric nanogenerator as energy-harvesting skin for self-powered electronics, *Nano Energy*, 2017, **39**, 429–436.
247 B. U. Ye, *et al.*, Electrospun ion gel nanofibers for flexible triboelectric nanogenerator: electrochemical effect on output power, *Nanoscale*, 2015, **7**, 16189–16194.
248 D. Bao, *et al.*, An anti-freezing hydrogel based stretchable triboelectric nanogenerator for biomechanical energy harvesting at sub-zero temperature, *J. Mater. Chem. A*, 2020, **8**, 13787–13794.
249 J. Jin, H. Ma, H. Liang and Y. Zhang, Biopolymer-Derived Carbon Materials for Wearable Electronics, *Adv. Mater.*, 2025, **37**, 2414620.
250 D. Wirthl, *et al.*, Instant tough bonding of hydrogels for soft machines and electronics, *Sci. Adv.*, 2017, **3**, e1700053.
251 C. Chiang Foo, *et al.*, Performance of dissipative dielectric elastomer generators, *J. Appl. Phys.*, 2012, **111**, 094107.
252 S. J. A. Koh, X. Zhao and Z. Suo, Maximal energy that can be converted by a dielectric elastomer generator, *Appl. Phys. Lett.*, 2009, **94**, 262902.
253 J. Huang, S. Shian, Z. Suo and D. R. Clarke, Maximizing the energy density of dielectric elastomer generators using equi-biaxial loading, *Adv. Funct. Mater.*, 2013, **23**, 5056–5061.
254 S. J. A. Koh, C. Keplinger, T. Li, S. Bauer and Z. Suo, Dielectric elastomer generators: How much energy can be converted?, *IEEE/ASME Trans. Mechatron.*, 2010, **16**, 33–41.
255 Y. Zhou and L. Jiang, Bioinspired Nanoporous Membrane for Salinity Gradient Energy Harvesting, *Joule*, 2020, **4**, 2244–2248.
256 Z. Zhang, L. Wen and L. Jiang, Nanofluidics for osmotic energy conversion, *Nat. Rev. Mater.*, 2021, 1–18.
257 T. B. Schroeder, *et al.*, An electric-eel-inspired soft power source from stacked hydrogels, *Nature*, 2017, **552**, 214–218.
258 Z. Zhang, *et al.*, Improved osmotic energy conversion in heterogeneous membrane boosted by three-dimensional hydrogel interface, *Nat. Commun.*, 2020, **11**, 875.
259 W. Wang, *et al.*, Electron-ion coupling enables ionic hydrogel with high thermopower for low-grade heat harvest and sensitive fire warning, *J. Mater. Chem. A*, 2025, **13**, 30180–30190.
260 Y. Chen, C. Ye, J. He, L. Qu and S. Tang, Ion-engine hydrogel based solar desalination for water-electricity cogeneration with milliampere level current, *Nat. Commun.*, 2025, **16**, 10321.
261 F. Xin and Q. Lyu, A review on thermal properties of hydrogels for electronic devices applications, *Gels*, 2022, **9**, 7.
262 T. Li, *et al.*, Dual-ionic hydrogels with ultralong anti-dehydration lifespan and superior anti-icing performance, *Appl. Mater. Today*, 2022, **26**, 101367.
263 S. Yang, *et al.*, Dehydration drives damage in the freezing of brittle hydrogels, *Sci. Adv.*, 2024, **10**, eado7750.
264 X. Zhao, A. Shi, L. Shi, W. Sun and Z. You, An Overview of Recent Advances in Antidehydration and Antifreezing Hydrogels, *ACS Appl. Energy Mater.*, 2025, **8**, 13020–13039.

265 J. H. Kim, *et al.*, Multiscale Engineering of Ion-Conducting Gels for Sustainable Bioelectronic Systems, *Small Methods*, 2026, **10**, e01625.
266 Y. Lei, *et al.*, Polyanionic hydrogel electrolytes to regulate ion transport behavior in long cycle life zinc-ion batteries, *Nano Energy*, 2025, **143**, 111284.
267 K. Wang, *et al.*, Flexible and stable n-isopropylacrylamide/sodium alginate gel electrolytes for aqueous Zn-MnO2 batteries, *Batteries*, 2023, **9**, 426.
268 D. Zhong, *et al.*, A strategy for tough and fatigue-resistant hydrogels via loose cross-linking and dense dehydration-induced entanglements, *Nat. Commun.*, 2024, **15**, 5896.
269 A. H. Karoyo and L. D. Wilson, A review on the design and hydration properties of natural polymer-based hydrogels, *Materials*, 2021, **14**, 1095.
270 J. P. Gong, Y. Katsuyama, T. Kurokawa and Y. Osada, Double-network hydrogels with extremely high mechanical strength, *Adv. Mater.*, 2003, **15**, 1155–1158.
271 R. Zhu, D. Zhu, Z. Zheng and X. Wang, Tough double network hydrogels with rapid self-reinforcement and low hysteresis based on highly entangled networks, *Nat. Commun.*, 2024, **15**, 1344.
272 J. Berger, *et al.*, Structure and interactions in covalently and ionically crosslinked chitosan hydrogels for biomedical applications, *Eur. J. Pharm. Biopharm.*, 2004, **57**, 19–34.
273 K. J. Henderson, T. C. Zhou, K. J. Otim and K. R. Shull, Ionically cross-linked triblock copolymer hydrogels with high strength, *Macromolecules*, 2010, **43**, 6193–6201.
274 S. Lin, *et al.*, Anti-fatigue-fracture hydrogels, *Sci. Adv.*, 2019, **5**, eaau8528.
275 R. Bai, J. Yang, X. P. Morelle and Z. Suo, Flaw-Insensitive Hydrogels under Static and Cyclic Loads, *Macromol. Rapid Commun.*, 2019, **40**, 1800883.
276 Y. Okumura and K. Ito, The polyrotaxane gel: A topological gel by figure-of-eight cross-links, *Adv. Mater.*, 2001, **13**, 485–487.
277 Z. Shen, Q. Liang, Q. Chang, Y. Liu and Q. Zhang, Topological Hydrogels for Long-Term Brain Signal Monitoring, Neuromodulation, and Stroke Treatment, *Adv. Mater.*, 2024, **36**, 2310365.
278 T. Sakai, *et al.*, Design and fabrication of a high-strength hydrogel with ideally homogeneous network structure from tetrahedron-like macromonomers, *Macromolecules*, 2008, **41**, 5379–5384.
279 C. Zhao, *et al.*, Layered nanocomposites by shear-flow-induced alignment of nanosheets, *Nature*, 2020, **580**, 210–215.
280 B. He, *et al.*, Strain-coupled, crystalline polymer-inorganic interfaces for efficient magnetoelectric sensing, *Science*, 2025, **389**, 623–631.
281 Z.-G. Zhao, Y.-C. Xu, R.-C. Fang and M.-J. Liu, Bioinspired adaptive gel materials with synergistic heterostructures, *Chin. J. Polym. Sci.*, 2018, **36**, 683–696.
282 N. Oliva, J. Conde, K. Wang and N. Artzi, Designing hydrogels for on-demand therapy, *Acc. Chem. Res.*, 2017, **50**, 669–679.
283 X. Q. Dou and C. L. Feng, Amino acids and peptide-based supramolecular hydrogels for three-dimensional cell culture, *Adv. Mater.*, 2017, **29**, 1604062.
284 Z. Zhao, R. Fang, Q. Rong and M. Liu, Bioinspired nanocomposite hydrogels with highly ordered structures, *Adv. Mater.*, 2017, **29**, 1703045.
285 Z. Zhao, *et al.*, Biphasic synergistic gel materials with switchable mechanics and self-healing capacity, *Angew. Chem., Int. Ed.*, 2017, **56**, 13464–13469.
286 Z. Zhao, *et al.*, Dual-programmable shape-morphing and self-healing organohydrogels through orthogonal supramolecular heteronetworks, *Adv. Mater.*, 2018, **30**, 1804435.
287 S. Zhuo, *et al.*, Complex multiphase organohydrogels with programmable mechanics toward adaptive soft-matter machines, *Sci. Adv.*, 2020, **6**, eaax1464.
288 G. Shin, *et al.*, Mechanically Adaptable High-Performance p (SBMA-MMA) Copolymer Hydrogel with Iron (II/III) Perchlorate for Wearable Thermocell Applications, *Adv. Funct. Mater.*, 2025, **35**, 2412524.
289 M. A. C. Stuart, *et al.*, Emerging applications of stimuli-responsive polymer materials, *Nat. Mater.*, 2010, **9**, 101–113.
290 O. Yasa, *et al.*, An overview of soft robotics, *Annu. Rev. Control Robot. Auton. Syst.*, 2023, **6**, 1–29.
291 B. Li, M. Li and Y. Wang, Smart hydrogels in wearable electronics for wound treatments, *Small*, 2025, **21**, e07368.
292 S. Wang and M. W. Urban, Self-healing polymers, *Nat. Rev. Mater.*, 2020, **5**, 562–583.
293 R. F. Diegelmann and M. C. Evans, Wound healing: an overview of acute, fibrotic and delayed healing, *Front. Biosci.*, 2004, **9**, 283–289.
294 A. Biggs, Suberized boundary zones and the chronology of wound response in tree bark, *Phytopathology*, 1985, **75**, 1191–1195.
295 D. L. Taylor and M. Het Panhuis, Self-healing hydrogels, *Adv. Mater.*, 2016, **28**, 9060–9093.
296 B. J. Blaiszik, *et al.*, Self-healing polymers and composites, *Annu. Rev. Mater. Res.*, 2010, **40**, 179–211.
297 Z. Wei, *et al.*, Self-healing gels based on constitutional dynamic chemistry and their potential applications, *Chem. Soc. Rev.*, 2014, **43**, 8114–8131.
298 M. C. Roberts, M. C. Hanson, A. P. Massey, E. A. Karren and P. F. Kiser, Dynamically restructuring hydrogel networks formed with reversible covalent crosslinks, *Adv. Mater.*, 2007, **19**, 2503–2507.
299 G. Deng, *et al.*, Dynamic hydrogels with an environmental adaptive self-healing ability and dual responsive sol–gel transitions, *ACS Macro Lett.*, 2012, **1**, 275–279.
300 Y. Amamoto, H. Otsuka, A. Takahara and K. Matyjaszewski, Self-healing of covalently cross-linked polymers by reshuffling thiuram disulfide moieties in air under visible light, *Adv. Mater.*, 2012, **24**, 3975–3980.
301 Y. Zhang, L. Tao, S. Li and Y. Wei, Synthesis of multi-responsive and dynamic chitosan-based hydrogels for controlled release of bioactive molecules, *Biomacromolecules*, 2011, **12**, 2894–2901.

302 Y. Zhang, *et al.*, A magnetic self-healing hydrogel, *Chem. Commun.*, 2012, **48**, 9305–9307.
303 W. G. Skene and J.-M. P. Lehn, Dynamers: polyacylhydrazone reversible covalent polymers, component exchange, and constitutional diversity, *Proc. Natl. Acad. Sci. U. S. A.*, 2004, **101**, 8270–8275.
304 T. Maeda, H. Otsuka and A. Takahara, Dynamic covalent polymers: Reorganizable polymers with dynamic covalent bonds, *Prog. Polym. Sci.*, 2009, **34**, 581–604.
305 F. Yu, X. Cao, J. Du, G. Wang and X. Chen, Multifunctional hydrogel with good structure integrity, self-healing, and tissue-adhesive property formed by combining Diels–Alder click reaction and acylhydrazone bond, *ACS Appl. Mater. Interfaces*, 2015, **7**, 24023–24031.
306 B. Briou, B. Améduri and B. Boutevin, Trends in the Diels–Alder reaction in polymer chemistry, *Chem. Soc. Rev.*, 2021, **50**, 11055–11097.
307 T.-A. Asoh, W. Kawai and A. Kikuchi, Alternating-current electrophoretic adhesion of biodegradable hydrogel utilizing intermediate polymers, *Colloids Surf., B*, 2014, **123**, 742–746.
308 A. Phadke, *et al.*, Rapid self-healing hydrogels, *Proc. Natl. Acad. Sci. U. S. A.*, 2012, **109**, 4383–4388.
309 P. Li, *et al.*, Hydrogen bond network connectivity in the electric double layer dominates the kinetic pH effect in hydrogen electrocatalysis on Pt, *Nat. Catal.*, 2022, **5**, 900–911.
310 D. C. Tuncaboylu, M. Sari, W. Oppermann and O. Okay, Tough and self-healing hydrogels formed via hydrophobic interactions, *Macromolecules*, 2011, **44**, 4997–5005.
311 T. Kakuta, *et al.*, Preorganized hydrogel: self-healing properties of supramolecular hydrogels formed by polymerization of host-guest-monomers that contain cyclodextrins and hydrophobic guest groups, *Adv. Mater.*, 2013, **25**, 2849–2853.
312 Z. Wei, *et al.*, Autonomous self-healing of poly (acrylic acid) hydrogels induced by the migration of ferric ions, *Polym. Chem.*, 2013, **4**, 4601–4605.
313 K. Haraguchi, R. Farnworth, A. Ohbayashi and T. Takehisa, Compositional effects on mechanical properties of nanocomposite hydrogels composed of poly (N, N-dimethylacrylamide) and clay, *Macromolecules*, 2003, **36**, 5732–5741.
314 V. K. Kotharangannagari, A. Sánchez-Ferrer, J. Ruokolainen and R. Mezzenga, Photoresponsive reversible aggregation and dissolution of rod–coil polypeptide diblock copolymers, *Macromolecules*, 2011, **44**, 4569–4573.
315 J. Xu and P. Chen, Effect of crystallization behavior and phase evolution on glass-ceramics derived from alumina silicate solid waste with addition high content CaF2, *Chem. Eng. J.*, 2025, **506**, 159998.
316 Y. Xu, Q. Wu, Y. Sun, H. Bai and G. Shi, Three-dimensional self-assembly of graphene oxide and DNA into multifunctional hydrogels, *ACS Nano*, 2010, **4**, 7358–7362.
317 R. Chen, *et al.*, Temperature-regulated flexibility of polymer chains in rapidly self-healing hydrogels, *NPG Asia Mater.*, 2019, **11**, 22.
318 J. C. Yang, *et al.*, Electronic skin: recent progress and future prospects for skin-attachable devices for health monitoring, robotics, and prosthetics, *Adv. Mater.*, 2019, **31**, 1904765.
319 Z. Lei and P. Wu, Adaptable polyionic elastomers with multiple sensations and entropy-driven actuations for prosthetic skins and neuromuscular systems, *Mater. Horiz.*, 2019, **6**, 538–545.
320 H. Guo, *et al.*, All-in-one shape-adaptive self-charging power package for wearable electronics, *ACS Nano*, 2016, **10**, 10580–10588.
321 H. Huang, *et al.*, Super-stretchable, elastic and recoverable ionic conductive hydrogel for wireless wearable, stretchable sensor, *J. Mater. Chem. A*, 2020, **8**, 10291–10300.
322 X. Du, *et al.*, Reconfiguration, camouflage, and color-shifting for bioinspired adaptive hydrogel-based millirobots, *Adv. Funct. Mater.*, 2020, **30**, 1909202.
323 Y. Kim, H. Yuk, R. Zhao, S. A. Chester and X. Zhao, Printing ferromagnetic domains for untethered fast-transforming soft materials, *Nature*, 2018, **558**, 274–279.
324 H. Yuk, T. Zhang, G. A. Parada, X. Liu and X. Zhao, Skin-inspired hydrogel–elastomer hybrids with robust interfaces and functional microstructures, *Nat. Commun.*, 2016, **7**, 12028.
325 Y. Yu, *et al.*, Multifunctional ''hydrogel skins'' on diverse polymers with arbitrary shapes, *Adv. Mater.*, 2019, **31**, 1807101.
326 B. Yu, *et al.*, Use of hydrogel coating to improve the performance of implanted glucose sensors, *Biosens. Bioelectron.*, 2008, **23**, 1278–1284.
327 M. Shin, *et al.*, Complete prevention of blood loss with self-sealing haemostatic needles, *Nat. Mater.*, 2017, **16**, 147–152.
328 T. Zhao, *et al.*, Macroscopic layered organogel–hydrogel hybrids with controllable wetting and swelling performance, *Adv. Funct. Mater.*, 2018, **28**, 1800793.
329 H. Yuk, T. Zhang, S. Lin, G. A. Parada and X. Zhao, Tough bonding of hydrogels to diverse non-porous surfaces, *Nat. Mater.*, 2016, **15**, 190–196.
330 Q. Liu, G. Nian, C. Yang, S. Qu and Z. Suo, Bonding dissimilar polymer networks in various manufacturing processes, *Nat. Commun.*, 2018, **9**, 846.
331 W. Shi, *et al.*, Cellular-skeleton-hosting polymer fluid gels with high damping and mechanical stability over an ultra-wide frequency breadth, *Matter*, 2025, **8**(12), 102373.
332 J. Huang, *et al.*, Ultrahigh energy-dissipation elastomers by precisely tailoring the relaxation of confined polymer fluids, *Nat. Commun.*, 2021, **12**, 3610.
333 H. Kamata, Y. Akagi, Y. Kayasuga-Kariya, U.-I. Chung and T. Sakai, ''Nonswellable'' hydrogel without mechanical hysteresis, *Science*, 2014, **343**, 873–875.
334 J. Xu, R. Jin, X. Ren and G. Gao, Cartilage-inspired hydrogel strain sensors with ultrahigh toughness, good self-recovery and stable anti-swelling properties, *J. Mater. Chem. A*, 2019, **7**, 25441–25448.
335 H. Gao, *et al.*, Adaptive and freeze-tolerant heteronetwork organohydrogels with enhanced mechanical

stability over a wide temperature range, *Nat. Commun.*, 2017, **8**, 15911.
336 R. Wang, C. Cheng, H. Wang and D. Wang, Swollen hydrogel nanotechnology: Advanced applications of the rudimentary swelling properties of hydrogels, *ChemPhysMater*, 2024, **3**, 357–375.
337 Q. Wu, S. Qi, T. Zhao, H. Yan and M. Liu, Multiple network organohydrogels with high strength and anti-swelling properties in different solvents, *Giant*, 2021, **6**, 100058.
338 P. Lin, S. Ma, X. Wang and F. Zhou, Molecularly engineered dual-crosslinked hydrogel with ultrahigh mechanical strength, toughness, and good self-recovery, *Adv. Mater.*, 2015, **27**, 2054–2059.
339 H. Fan, J. Wang and Z. Jin, Tough, swelling-resistant, self-healing, and adhesive dual-cross-linked hydrogels based on polymer–tannic acid multiple hydrogen bonds, *Macromolecules*, 2018, **51**, 1696–1705.
340 Y. Zhang, *et al.*, Multiple hydrogen bonds enable high strength and anti-swelling cellulose-based ionic conductive hydrogels for flexible sensors, *Chem. Eng. J.*, 2024, **480**, 148318.
341 Y. Xu, Q. Rong, T. Zhao and M. Liu, Anti-Freezing multiphase gel materials: Bioinspired design strategies and applications, *Giant*, 2020, **2**, 100014.
342 X. P. Morelle, *et al.*, Highly stretchable and tough hydrogels below water freezing temperature, *Adv. Mater.*, 2018, **30**, 1801541.
343 Y. Bai, *et al.*, Transparent hydrogel with enhanced water retention capacity by introducing highly hydratable salt, *Appl. Phys. Lett.*, 2014, **105**(15), 151903.
344 X. Li, *et al.*, Low-temperature ionic conductivity enhanced by disrupted ice formation in polyampholyte hydrogels, *Macromolecules*, 2018, **51**, 2723–2731.
345 X. F. Zhang, *et al.*, Inorganic salts induce thermally reversible and anti-freezing cellulose hydrogels, *Angew. Chem., Int. Ed.*, 2019, **58**, 7366–7370.
346 L. Han, *et al.*, Mussel-inspired adhesive and conductive hydrogel with long-lasting moisture and extreme temperature tolerance, *Adv. Funct. Mater.*, 2018, **28**, 1704195.
347 J. C. Rasaiah, S. Garde and G. Hummer, Water in nonpolar confinement: from nanotubes to proteins and beyond, *Annu. Rev. Phys. Chem.*, 2008, **59**, 713–740.
348 K. Mochizuki and K. Koga, Solid– liquid critical behavior of water in nanopores, *Proc. Natl. Acad. Sci. U. S. A.*, 2015, **112**, 8221–8226.
349 P. Le Floch, *et al.*, Wearable and washable conductors for active textiles, *ACS Appl. Mater. Interfaces*, 2017, **9**, 25542–25552.
350 H. Peng and Q. Zhao, A nano-heterogeneous membrane for efficient separation of lithium from high magnesium/lithium ratio brine, *Adv. Funct. Mater.*, 2021, **31**, 2009430.
351 B. Yao, *et al.*, Hydrogel ionotronics with ultra-low impedance and high signal fidelity across broad frequency and temperature ranges, *Adv. Funct. Mater.*, 2022, **32**, 2109506.
352 Z. Wu and Z. Zhao, Heterogating gel iontronics: a revolution in biointerfaces and ion signal transmission, *Gels*, 2024, **10**, 594.
353 X. He, *et al.*, Highly conductive and stretchable nanostructured ionogels for 3D printing capacitive sensors with superior performance, *Nat. Commun.*, 2024, **15**, 6431.
354 E. M. Stewart, S. Narayan and L. Anand, An electro-chemo-mechanical theory for hydrogel ionotronics: Application to modeling a capacitive strain sensor and a dynamic large strain actuator, *J. Mech. Phys. Solids*, 2023, **173**, 105196.